1991

Fatigue and corrosion fatigue of smooth and notched Be-Cu spring materials

Reza Bagheri
Lehigh University

Fatigue and Corrosion Fatigue
of
Smooth and Notched Be-Cu Spring Materials

by

Reza Bagheri

A Thesis
Presented to the Graduate Committee
of Lehigh University
in Candidacy for the Degree of Master of Science
in
Materials Science and Engineering

Lehigh University
1991

CERTIFICATE OF APPROVAL

Approved and recommended for acceptance as a thesis in partial fulfilment of the requirements for the degree of Master of Science.

September 3, 1991
Date

Gary A. Miller
Professor in Charge

Richard Wolfson
Chairperson of the Department

ACKNOWLEDGEMENTS

I would like to thank my advisor, Dr. Gary A. Miller, and my co-advisor, Dr. Clifford C. Hanninen, for providing a nice program in the fatigue area that extended a lot my knowledge and feeling about the mechanical behavior of metals. Their advice and guidance in the course of this study is greatly appreciated.

Thanks are also due to my friends Hamid R. Azimi, Thomas C. Clark, and Thomas J. Pecorini for their supporting through technical discussions. Technicians Jack Williams, Gene Kozma, Kathy Repa, and Dave Ackland were of great help in this effort — I thank them all.

I appreciate NGK Metals Co. for providing materials and support of this work. Thanks also go to Mr. W. Drew Peregrim for obtaining part of materials used. I would also like to appreciate Iranian Ministry of Culture and Higher Education for providing personal financial support.

Lastly, I would be glad to acknowledge my wife, Nazanin, for her patience and encouragement during this time, and my son, Mostafa, for being patient in the absence of father.

TABLE OF CONTENTS

LIST OF FIGURES

LIST OF TABLES

ABSTRACT

Fine gage springs, i.e., 0.001 to 0.010 inch thick, of Be-Cu are used as electrical connectors at a rate of millions of pounds per year in the world market. Lack of knowledge on fatigue and corrosion fatigue behavior of Be-Cu led to a reaserch effort to generate needed data. Special circumstances which are associated with the size of these connectors, e.g., resonance in fatigue cycling and buckling made this effort more difficult and complex.

Cold work and heat treatment were studied in this research as two important production treatments. Notches were also introduced to represent unavoidable geometrical discontinuties. Some tests were conducted in 0.5N salt water to study corrosion fatigue of Be-Cu alloy. Transmission and scanning electron microscopy were also employed to characterize the alloy performance.

Cyclic softening and hardening were found in fatigue of cold worked and annealed Be-Cu, respectively. The latter was associated with cyclic strain aging. A 120% increase in flow strength of the annealed material after 2×10^6 fatigue cycles was observed. It was shown that any mechanical or thermal treatment that decreases the ductility of the material, increases the notch sensitivity.

In contrast to published literature showing excellent corrosion fatigue behavior of Be-Cu, a considerable decrease in fatigue strength of this material in the aged condition was found. These observations are rationalized by the fact that the test frequency in this investigation was 1 Hz, while the published data on corrosion fatigue of Be-Cu are for tests at 20 Hz or higher. Deleterious effects of both notch and corrosive environment were found to be greater at high, i.e. 10^6, cycles than for low, i.e. 10^4, cycles. Much less environmental sensitivity was observed in the presence of a notch in compared with that observed in the absence of a notch.

1. INTRODUCTION

Beryllium copper, also called Be bronze, has many excellent characteristics. It is among the hardest and strongest of all the copper-base alloys[1]. Since the early decades of the 20th century, beryllium copper has been used in many engineering applications in the form of both castings and wrought products. Since that time, beryllium copper components have been produced for ship propellers, oil drilling, jet aircraft landing gear, wind tunnel apparatus, molds for producing plastic parts, submarine telephone equipment, electrical connectors, etc. Fine gage strips, say 0.001 to 0.010 inch thick, of beryllium copper are produced through a combination of solution annealing, cold forming, and age hardening. These strips are used for electrical and electronic devices in a very high volume, i.e. millions of pounds per year, in the world market. These electrical and electronic connectors are in the form of springs and consequently their fatigue behavior has been of great interest among the producers and consumers. In service, these connectors are sometimes exposed to corrosive environments, which underscores the importance of determining their fatigue behavior in aqueous as well as ambient environments.

Corrosion fatigue or *environmentally assisted fatigue cracking* is a term used to describe the phenomenon of gradual accumulation of damage in a material under the combined actions of a fluctuating stress (fatigue) and a corrosive environment. This process causes alterations in crack initiation, crack propagation, and fracture of the material. All structural metals including aluminum, titanium, copper, and ferrous alloys are susceptible to corrosion fatigue. The degree of damage which occurs depends upon the relative aggresiveness of the environment, cyclic loading conditions, temperature, etc. The fatigue life may be reduced to a fraction of its ambient value in the presence of an aggressive environment[2,3]. Corrosion fatigue, due to the nature of corrosion, is a time dependent phenomenon. Therefore, the lower the frequency of load fluctuations, the greater is the time of exposure, and the greater the environmental influence. Generally speaking, corrosion fatigue is the most common mode of fracture due to combination of mechanical loading and environmental interaction[4].

The published literature contains very few investigations[5-7] on corrosion fatigue of Be-Cu. Gough and Sopwith[5] found excellent fatigue properties for beryllium copper

in both fresh water and brine, comparable to that of 18-8 stainless steel. In an investigation on corrosion resistance of Be-Cu, Richards[6] reported an excellent resistance to corrosion, stress corrosion, and corrosion fatigue of Be-Cu when it was exposed to 3% salt water spray. He examined solution treated, cold drawn, and aged beryllium copper and observed nearly no change in fatigue life under corrosive conditions. Reviewing the literature, Jaske et al[8] also reported that the wrought Be-Cu has the highest corrosion fatigue strength value of all the copper alloys in salt water. An interesting point in all these investigations is that all data reported on corrosion fatigue of beryllium copper are from tests done at high frequencies, i.e., 20-40 Hz. This means that the time for corrosion has been relatively short in all these studies.

Design requirements for different applications of thin gage materials, as well as any engineering material, will inevitably leads to stress raisers in products which act like notches. Despite the importance of notches on fatigue behavior, no data were found on notch effects on both fatigue and corrosion fatigue of Be-Cu.

Finally, the importance of processing variables such as cold forming and heat treatment, besides the absence of data on the notch effect on fatigue behavior in ambient and aqueous environment of beryllium copper suggests the need for a research effort in this field. It is important to understand both microscopic and macroscopic aspects of fatigue in the Be-Cu alloy system.

1.1 Fatigue Damage

1.1.1 Ambient Air Fatigue

Fatigue damage is accompanied by local plastic deformation whether the nominal applied stress is below or above the unidirectional yield stress. This plastic defomation occurs at stress raisers, e.g., rough surfaces, and involves the formation of slip bands. These slip bands appear on the surface of the fatigued material. Consequently, extrusions and intrusions form in these bands and the intrusions become the source of crack initiation[9-13]. Most researchers have reported that fatigue cracks initiate on the surface of the cyclically loaded specimens. However, some sub-surface crack initiation has been reported[14,15]. This sub-surface initiation occurs when a strongly adherent metal surface oxide exists which retards initiation at the external surface. Several fatigue crack initiation models have been proposed, all of them based on the slip on crystallographic planes[3]. The differences between these models relate to the slip character of different materials which can be slip on a single system, on the alternating parallel slip planes, and on the multiple slip systems. According to these models, the fatigue crack initates from the deepened intrusions and tends to follow specific crystallographic planes for a while. Later the crack formed grows in a plane perpendicular to the applied load direction[16]. Non-reversible plastic deformation occurs in front of the crack tip during the crack propagation process in a manner similar to that of crack nucleation[3]. Obviously the importance of the role of slip mechanism on fatigue crack initiation and propagation depends upon the ability of the material to undergo plastic deformation. It is why the mechanisms proposed on the basis of slip are much more applicable to ductile materials[3].

1.1.2 Corrosion Fatigue

As mentioned before, the presence of an aggressive environment, usually, decreases the fatigue life of the metals. This effect is due to the interaction between localized cyclic deformation and chemical reaction which can affect both initiation and propagation stages[3,17-19]. In the case of smooth polished specimens, Sudarshan et al[3] reported up to a nine times reduction in fatigue crack initiation life upon exposure to

an aggressive environment. They equated the effect of such an environment to introducing of a sharp notch into the surface. They argued that a corrosive environment facilitates the formation of discontinuties on the surface which can later become fatigue cracks. Four major theories have been proposed for explaining fatigue damage in aqueous environments, these are:

• **Pitting** — This mechanism was one of the earliest theories proposed to explain the fatigue life reduction in aqueous environments. According to this theory, corrosion induced pits on the fatigue specimen surface act as stress raisers which facilitate the crack initiation process. Many studies on low-carbon steels have shown this phenomenon responsible for fatigue cracking in corrosive environments[19].

• **Protective Film Destruction** — When the electrochemical potential of a metal in a given aqueous environment is in the passive region, this mechanism becomes important. In such a case, the protective film can rupture due to mechanical loading. Therefore, a discontinuity form on the surface of the metal which acts as an origin for crack nucleation. The same mechanism can accelerate the crack propagation rate by preventing the formation of protective layer at crack tip. This mechanism has been observed in corrosion fatigue of mild steel, stainless steel, and aluminum alloys in sea water[3].

• **Strain Enhanced Dissolution of Slip Steps** — This mechanism has been found to be active in corrosion fatigue of copper and several copper alloys[3,19,20]. The origin of this model is that deformed areas in metals are anodic relative to undeformed regions[19]. This idea comes from the fact that atoms in deformed regions are in a higher energy state than the atoms in undeformed areas. Two contradictory statements have been reported as a consequence of this mechanism. Hahn and Duquette[20] observed an increase in slip offset height and density, but blunting of slip band cracks which resulted in delay in crack initiation and an increase in fatigue life of Cu and Al-Cu single crystals exposed to salt water. On the other hand, many investigations have shown[3,19] a premature fatigue crack initiation in aggressive environments. This accelerated crack nucleation has been attributed to the concentration of deformation in the slip bands which are preferentially corroded. Hahn and Duquette[21] observed that enhanced localized dissolution also alters the fatigue crack path from transcrystalline in air to either partially or totally intergranular in corrosive environment in a CuNiCr

alloy. They argued that surface softening and blunting of slip band cracks suppress crack initiatioin in slip bands. Instead, cracks initiate and grow at grain boundries, due to geometric constraint.

• **Surface Adsorption** — The surface energy of a metal can be reduced by adsorption of specific species from the environment. This phenomenon lowers the local bond energies and facilitates crack initiation and propagation[19]. Hydrogen embrittlement of metals which results in premature fatigue fracture is one example of this mechanism.

As shown in Figure 1.1, these four mechanisms are directly described by different regions in a polarization curve[3].

1.1.3 Effect of Dissolved Oxygen on Corrosion Fatigue

The importance of dissolved oxygen on corrosion fatigue has been reported by several investigators[22-25]. Mehdizadeh et al[23] observed 65% decrease of endurance limit when they fatigued AISI 1035 steel in aerated brine. They got no environmental effect when they repeated the same test in deaereated salt water. Working on corrosion fatigue of low-carbon steel in salt water, Duquette and Uhlig[24] also reported similar behavior. They observed rusting in regions of maximum stress in the solution containing dissolved oxygen. They related this observation to galvanic interaction of fresh metal at slip steps, formed by fatigue, with adjacent metal covered by the usual oxide films. In the other words, the region underneath the oxide film, but close to deformed area acts as anode in a galvanic cell and corrodes faster. Duquette and Uhlig[24] could compensate for the deleterious effect of aeration in their study by applying cathodic current.

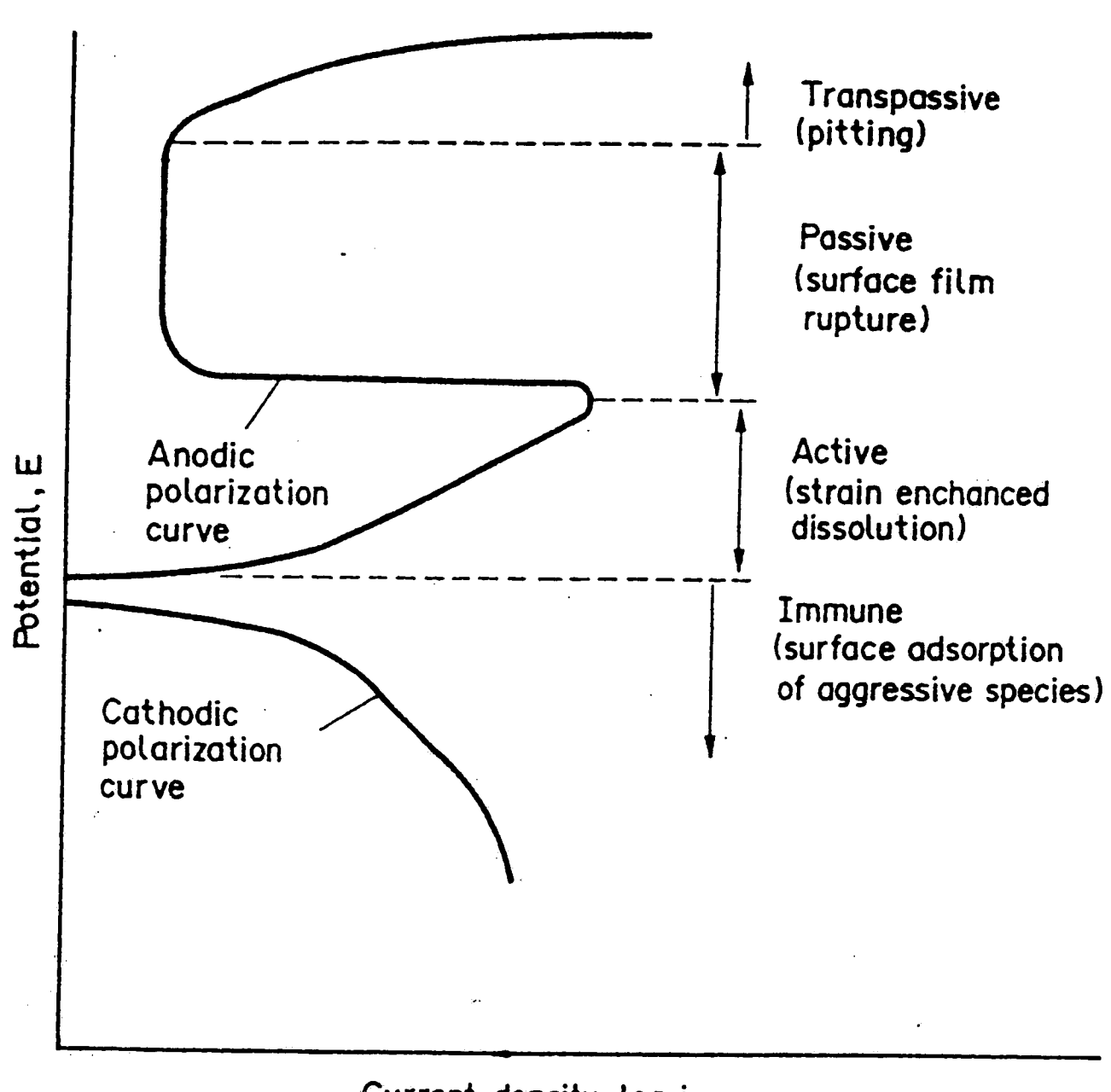

Figure 1.1. Correlation between regions of polarization and corrosion fatigue mechanisms[3].

1.2 Production Variables

1.2.1 Cold Work

Considering the nature of fatigue damage, i.e. the accumulation of deformation, it is expected that every treatment which increases the yield strength of the material, improves the fatigue strength. Generally speaking, cold working improves the cyclic behavior of metals. The influence of pre-deformation on fatigue resistance, similar to that of monotonic behavior, is due to introducing dislocations. The density of dislocations that exist in a metal prior to fatigue not only can affect the fatigue life, but can also cause cyclic softening or hardening[26]. Smith et al[27] proposed that the ratio of the monotonic ultimate tensile strength to the yield strength could be used to determine if softening or hardening would occur. They claimed that cyclic hardening is expected when this ratio is greater than 1.4, cyclic softening is dominant when it is less than 1.2, and no significant strength change is expected between 1.2 and 1.4. Studying the fatigue limit of copper, Awatani et al[28] observed cyclic hardening and softeninig in annealed and cold worked materials, respectively. They found that in pre-stretched copper, the dislocation substructures form in fatigue cycling. These networks then grow toward the grain boundries at high cycles and lead to formation of relatively dislocation free grains. The formation of relatively dislocation free grains is responsible for cyclic softening that does not let the specimen to show a fatigue limit. On the other hand, they observed forests of dislocations in annealed copper at high cycles concentrated inside the grains which were responsible for cyclic hardening and introducing of endurance limit.

Cold working as well as other strengthening mechanisms, increase the environmental sensitivity. Regions with a high density of dislocations are high energy areas prone to environmental attack. Increased sensitivity of pre-deformed metal in a corrosive medium not only affects the crack initiation, but facilitates the crack propagation rate as well[29].

1.2.2 Heat Treatment

High strength can be obtained in Be-Cu alloys by age hardening of solutionized or solutionized and cold worked materials. Aging makes the alloy stronger through the introduction of second phase precipitates. Similar to the effect of cold working, age hardening increases both fatigue strength and sensitivity to environmental attack. The interface of the precipitate and the matrix is a high energy region prone to accelerated corrosion in aggressive environments. Additionally, precipitates act as barriers to dislocation movements resulting to formation of more localized dislocation substructure than that of annealed material. These high energy areas increase the environmental sensitivity.

Richards[6] reported 15% decrease in fatigue strength of solution treated Be-Cu in salt water after 5×10^7 cycles, while he observed 18% reduction in fatigue strength in solution treated and aged condition of the same material. Hahn and Duquette[21] found no effect on fatigue behavior of solutionized CuNiCr when it was exposed to NaCl solution. At the same time they observed 11% reduction in fatigue strength of that material in brine. Considering the point that both of those investigations were performed at high frequencies, i.e. 20 Hz and higher, a much greater environmental effect is expected at lower frequencies.

Studying the fatigue fracture surface of CuNiCr, Hahn and Duquette[21] observed that in both solutionized and aged materials, crack initiates mostly at slip bands and propagates for a small period of time transgranularly. However, sometimes, intergranular crack initiation was observed in aged material. The fracture texture then changes to intergranular mode and follows the grain boundries. They attributed the transgranular crack initiation to "notch-peak topography caused by dislocation motion in persistent slip bands, after strain saturation has been reached". They argued that grain boundary precipitates are responsible for intergranular crack initiation in aged material. Similar results have been reported for pure copper[13,30]. A shift from mostly transgranular to mostly intergranular crack initiation, as environment is changed from air to salt water, have been reported for pure copper[13,30] and CuNiCr alloy[21]. This shift in fracture mode in corrosive environment has been attributed to blunting of slip band cracks due to localized dissolution. Consequently, instead of slip bands, cracks form at grain boundries. This is why corrosive environment intensifies the intergranular fracture mode. More interesting in these studies[13,21,30], is the fact that

crack initiation life of both solutionized and aged materials increased from approximately 5% to 40% of total fatigue life. Decreasing the total fatigue life and increasing the initiation life of copper and some of its alloys suggests that corrosion primarily affects the crack propagation rate. In the other words, there is a dynamic interaction at the crack tip between the corrosive media and the mechanical conditions that lead to accelerating fatigue crack growth.

1.3 Notch Effects

Most engineering components contain some change in geometry, discontinuities, or notches which act as stress raisers. The introduction of a notch to a sample under unidirectional loading results in a non-uniform stress distribution at the vicinity of the notch. The ratio of stress concentrated at the notch tip to the nominal stress applied is called the elastic stress concentration factor (K_t). Peterson[31] calculated K_t for many geometrical shapes.

Besides the high local stress, and consequently strain, introduced by the notch, the notch also results in a triaxial tensile state of stress in ductile materials. This triaxiality constrains the plastic deformation at notch tip which leads to increase in the yield strength. Therefore, ductile materials will be strengthened by introduction of the notch. On the other hand, when the material is brittle and does not tend to undergo plastic deformation at crack tip, the notched material breaks sooner than that of a smooth one and shows a lower strength due to the stress concentration[32]. The latter phenomenon is called notch weakening.

1.3.1 Notch Effects in Ambient Air Fatigue

Similar to what was discussed concerning monotonic behavior, a reduction in fatigue strength of materials is also expected in the presence of notch. This reduction is due to early initiation which is associated with the introduction of high stress field in the vicinity of notch. However, in some cases, it is possible that the growing crack stops when goes out of this high stress field.

The fatigue notch factor (K_f) is defined as as the ratio of fatigue strength of smooth sample divided by that of a notched one at a given life. In reality, the magnitude of the K_f is less than that of the K_t, meaning that the harmful effect of the notch on fatigue strength is less than that predicted from elasticity. This phenomenon can be attributed to the accumulation of plastic deformation at the notch tip, which decreases the deleterious effect of the high local stress. Frost et al[33] collected numbers of K_f-K_t relations proposed by others. These relations are mainly empirical and have been found for specific materials. Therefore, they are not applicable for every system. Note that K_t is based on geometry alone, while K_f accounts for both geometry and material characteristics. Among the various K_f-K_t relations, the one that is most widely used for different conditions is:

$$K_f = 1 + \frac{K_t - 1}{1 + \sqrt{A/\rho}} \qquad (1)$$

Where ρ is the notch root radius and A is a material constant. Some investigators have reported A as a function of tensile strength and/or yield strength of the material[33]. There are also some studies showing A as a function of grain size[34].

Almost none of the proposed K_f-K_t relations accounts for the effect of number of cycles to failure (N_f) on K_f. Collins[34] addressed studies confirming that K_f increases as N_f increases. The reason for this phenomenon is that as the stress decreases, the plastic deformation at notch tip decreases and elastic conditions are more closely approached. The extreme case of brittle behavior is when K_f reaches to K_t in a completely elastic material. Since K_f is close to 1 at one cycle, i.e., the tensile test, and increases with increasing N_f, it is usual to take K_f at 10^6—10^7 cycles to failure as the fatigue notch factor of the material.

The notch sensitivity factor (q) which is defined as the ratio of the changes of the actual stress range to the changes of the theoretical stress range, is a material constant[33]:

$$q = \frac{K_f - 1}{K_t - 1} \qquad (2)$$

It is known that for a given notch, the notch sensitivity increases as the strength of the material increases[35]. This effect is related to the more limited ability for deformation and crack blunting of the high strength materials which makes them more notch sensitive than that of ductile materials. Similar to what was mentioned in the case of K_f, an increase in the notch sensitivity factor (q) is expected as the number of cycles to failure increases.

1.3.2 Notch Effects in Corrosion Fatigue

Aggresive environments, as discussed before, can decrease the fatigue strength of the plain specimens. Therefore, it can be concluded that such an environment should have the same effect in the presence of notch. Frost et al[33] addressed several studies on notch effect in corrosive environments. These studies which have been conducted on different steels show that in the presence of a blunt notch, a moderate corrosive medium has the same effect on fatigue strength of both smooth and notched samples. Note that in the presence of a sharp notch, the crack initiates very soon and fatigue behavior is controlled by the stress required for crack growth and the rate of crack propagation. Therefore, in the case of sharp notches, environmental effect is mainly limited to its influence on propagation process, while in the case of blunt notches, the environment has its influence on both crack initiation and propagation stages.

Reviewing the literature, Miller[36] found that in some fatigue studies the notched fatigue strengths in an aqueous environment were superior to those in ambient

environment. These observations were related to the formation of a calcareous layer and to the cooling effect of the aqueous medium. Note that at high loads and for very high frequencies, the deleterious effect of a temperature rise, especially at crack tip, can be reduced by cooling effect of the aqueous solution.

Both Frost et al[33] and Miller[36] discussed studies confirming the absence of non-propagating cracks in notched steel samples exposed to corrosive environment. However, non-propagating cracks had been observed before in low-stress air fatigue testing of notched samples. These observations suggest that the stress level required to cause a crack to initiate and grow is lowered by some type of surface softening in the corrosive environment.

1.4 Objectives

The main objective of this study is to isolate and examine the effects of some of the major variables on the fatigue behavior of Be-Cu spring alloys. These variables include:

- Heat treatment and cold working as two important production treatments,
- Geometrical discontinuities as inevitable design requirements in engineering products,
- Aqueous medium representative of environmental influences.

The effects of these variables will be studied on the fatigue life under the stress control conditions. The results will be analyzed and compared with the theories and reports available in the literature. Microscopic aspects of fatigue will be also studied as a secondary goal in this investigation.

2. EXPERIMENTAL PROCEDURE

2.1 Materials

High strength and high conductivity Be-Cu spring materials, C17200 and C17500 respectively, were used in this study. Table 2.1 includes the specification for chemical composition, temper designation[37-39], grain size, and thickness of materials used. The materials obtained were in the form of strips with 0.75 inch in width.

Since some connectors are formed by bending age-hardened strips, alloy 10 in the aged condition was selected to study the effect of bending deformation on fatigue strength. The magnitude of the strain in bending of strips was measured using circle grid analysis method (Figure 2.1). Maximum strain measured in the tensile side of the bend was about 7%. Therefore, some samples of alloy 10 were stretched 7% prior to fatigue testing.

Three different conditions of alloy 25 were also used to study the effects of heat treatment and cold working.

2.1.1 Tensile Properties

Tensile samples were punched out of strips according to ASTM-E8[40]. Notched specimens were the same geometry as smooth samples except they contained a center hole of 0.047 inch diameter prepared using the electro-discharge machining (EDM) technique. An Instron 1011 testing machine was used for tensile tests under computer control. Tensile results summarized in Table 2.2 are for at least three samples for each smooth condition and two specimens for each notched condition.

Table 2.1. Be-Cu Materials and Composition

Alloy no.	UNS no.	Composition,wt%[1]	Temper Des.	GrainSize,μm[1]	Thickness,inch
25	C17200	Be = 1.85-1.9 Fe = 0.1-0.4 Si = 0.05-0.1 Al = 0.03-0.07 Co = 0.21-0.25 Ni = 0.03-0.06 Cu = Bal.	TBOO[2]	8-12	0.0063
			TDO4[3]	10-12	0.0062
			TMO4[4]	15	0.005
10	C17500	Be = 0.53 Fe = 0.03 Co = 2.61 Ni = 0.017 Cu = Bal.	TMO4[4]	10	0.006

1. According to material supplier report.
2. Solution heat treated (called annealed or solutionized in this report).
3. Solution heat treated and cold rolled (called cold rolled in this report).
4. Solution heat treated, cold rolled, and precipitation heat treated (called cold rolled and aged or aged in this report).

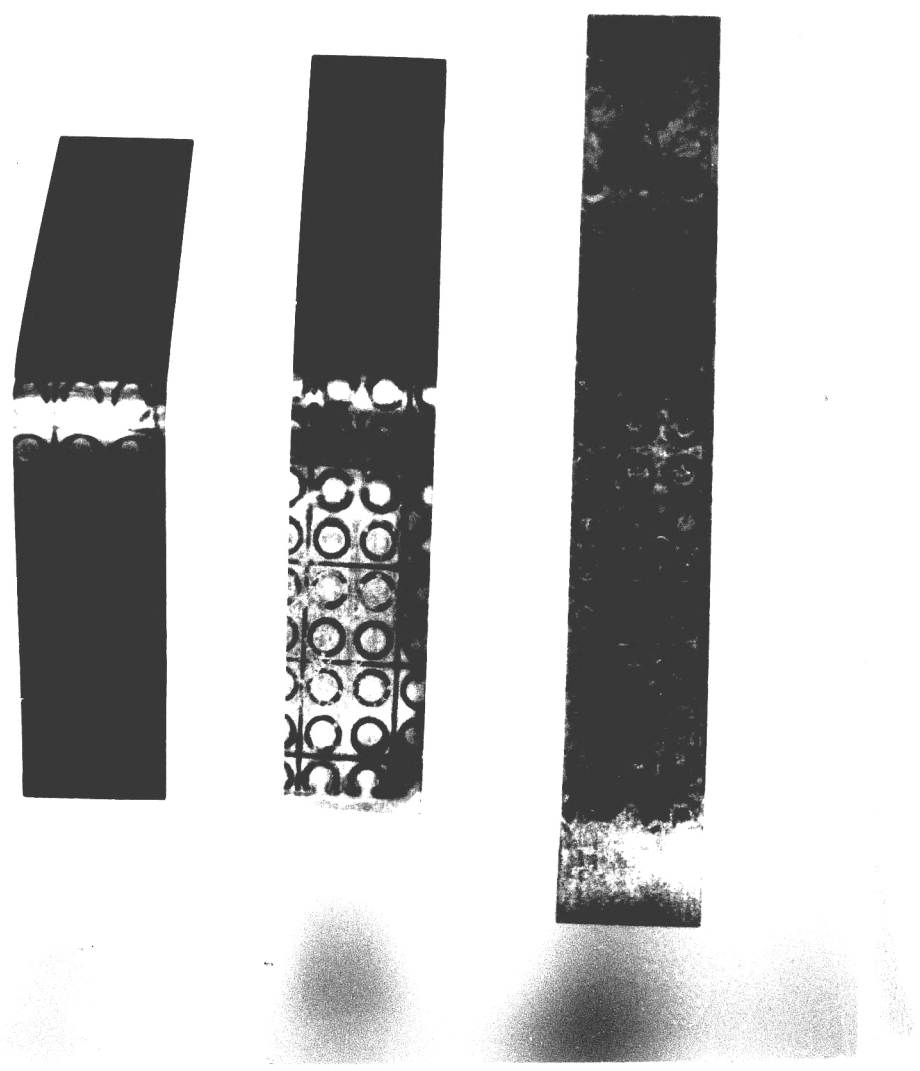

Figure 2.1. Diameter changes of electro-chemically printed grids represent the magnitude of the strain at the surface.

INTENTIONAL SECOND EXPOSURE

Figure 2.1. Diameter changes of electro-chemically printed grids represent the magnitude of the strain at the surface.

Table 2.2. Tensile Properties of Be-Cu materials.

Material I.D.	Smooth			Notched		
	S_y(ksi)	UTS(ksi)	El(%)*	S_y(ksi)	UTS(ksi)	El(%)*
10-TMO4	112.5	125.2	10	124.8	125	1.8
25-TBOO	31.1	69.8	42.3	36.6	61.7	12.7
25-TDO4	113.8	117.4	2.1	107	118.8	1.2
25-TMO4	115.3	145	16.8	132.8	134.9	1.7
Fatigued 25-TBOO	69.6	80.7	19.9	—	—	—

* Total elongation in 2 inches gage length.

Typical values for the standard deviation of yield strength, tensile strength, and %El were less than 4 ksi, 1.6 ksi, and 4%, respectively.

2.2 Fatigue Testing

Hour-glass fatigue specimens* were cut out of strips according to ASTM-E466[41] using EDM method. The specimens were cut with a radius of 4 inches to a minimum gage section width of 0.5 inch. Specimens of the same geometry except for a drilled center hole of 0.047 inch diameter were used as notched specimens.

Two and one half inch lengths of clear tygon tubing (1 inch outer diameter and 0.125 inch wall thickness) were glued to some smooth and notched samples of alloy 25 in both the annealed and the cold rolled and aged conditions as environmental chambers for corrosion tests. As seen in Figure 2.2, the tubing is closed at both ends and an opening is cut in the top to allow aeration of the aqueous environment.

The edges of all samples were polished using 600 grit sand paper prior to fatigue testing to remove possible irregularities due to the electro-discharge cutting process.

Load controlled fatigue tests were performed on a Instron closed-loop electro-hydraulic, Instron 2115, machine. All tests were conducted at ambient labratory temperature. A sinusoidal waveform and a minimum to maximum stress ratio of 0.1 were used in this fatigue testing program. The frequencies employed were up to 50 Hz for air fatigue and 1 Hz for corrosion fatigue experiments. Special grips (Figure 2.2) were designed to assure desired alignment. A guide plate was used to check the alignment of the grips prior to each test. The apparatus installed at the bottom grip in Figure 2.2 (bottom left), was designed to prevent any possible turning of the actuator during cycling. Note that in this type of fatigue frame, it is possible for the actuator to turn during cycling when the test sample is not stiff enough.

---

* Some preliminary fatigue tests were conducted on tensile samples of uniform gage section width. Most of these tests failed due to resonance of this geometry — a common occurence for thin materials subjected to fatigue cycling. The vibration was monitored using a strobelight. It could be limited somewhat by changing the frequency. However, at low frequencies required for corrosion tests, the vibration was worse. Consequently, it was necessary to change from a common tensile to an hour-glass shape to solve this problem. The hour-glass shape was found to be less susceptible to resonance than the standard tensile geometry.

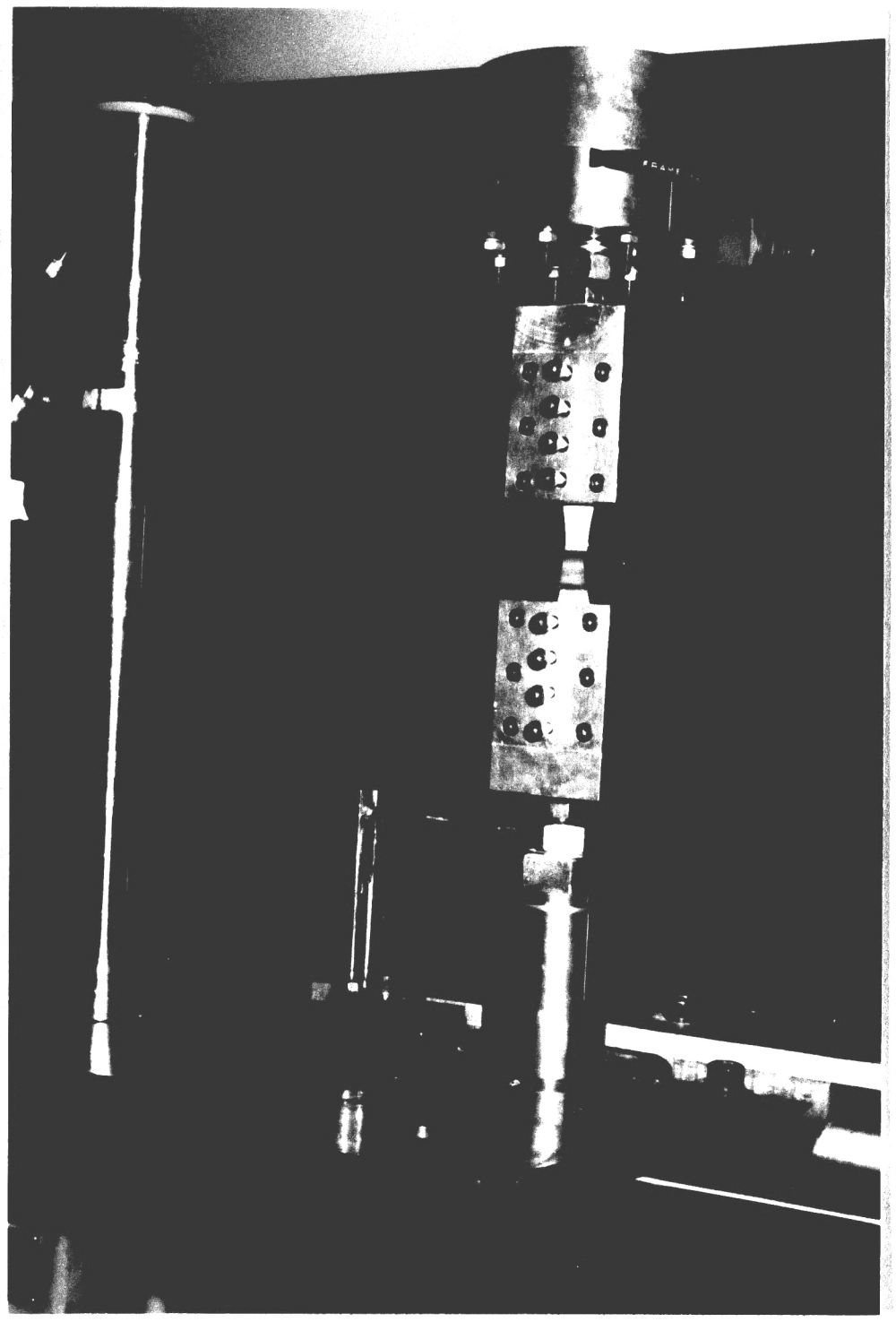

Figure 2.2. Fixturing for corrosion fatigue testing.

INTENTIONAL SECOND EXPOSURE

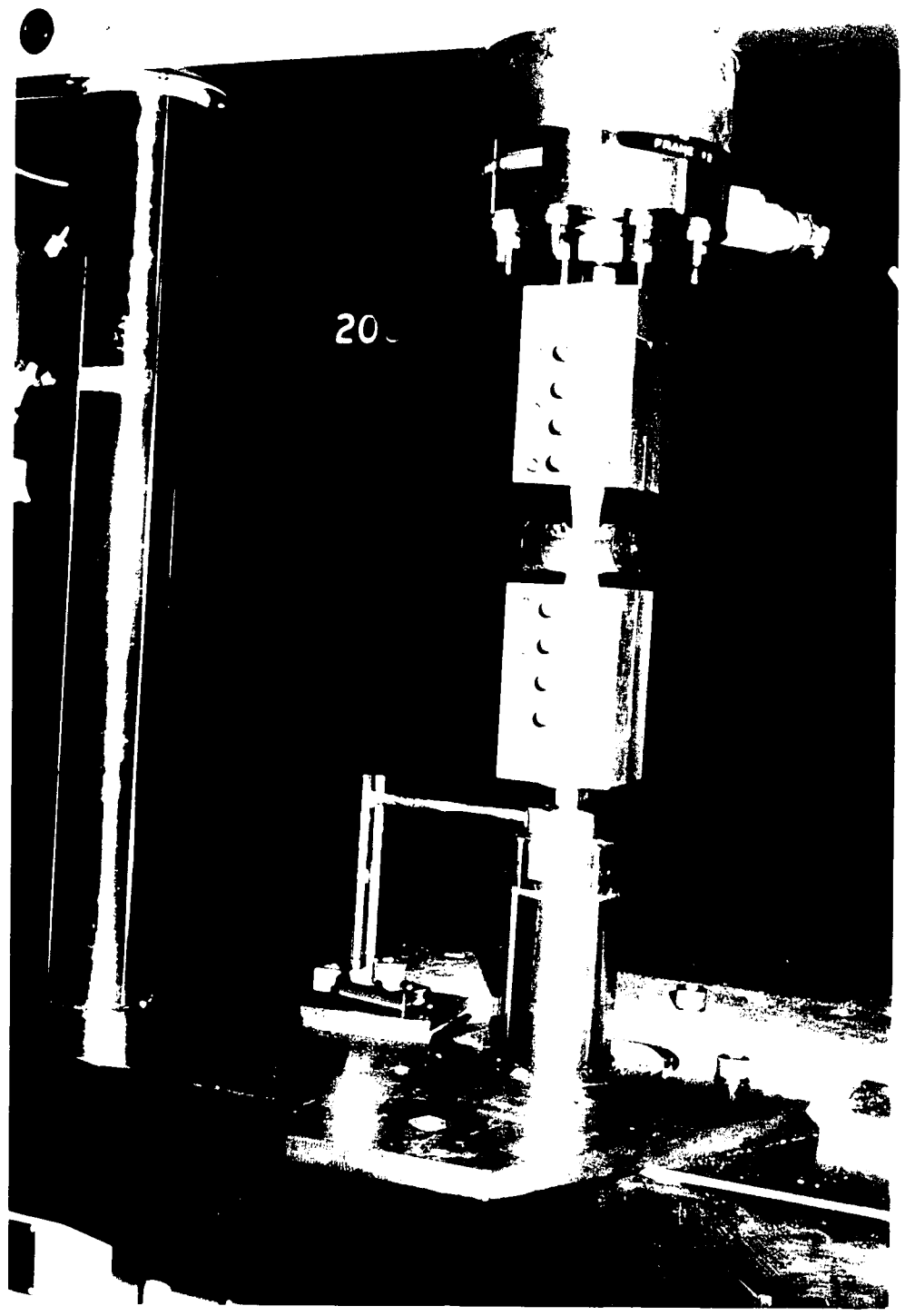

Figure 2.2. Fixturing for corrosion fatigue testing.

An 0.5N NaCl solution, i.e., 29.25 grams of sodium chloride in 1000 cm^3 of distilled water, was selected as the aqueous environment in the corrosion fatigue experiments. The pH of the solution measured at room temperature was 5.9.

2.3 Electron Microscopy

The fracture surface of some annealed and aged samples of alloy 25 tested in both ambient and aqueous environment were examined using an ETEC scanning electron microscope (SEM) at an accelerating voltage of 20 KV. Corrosion fatigue specimens were ultrasonically cleaned in Alconox solution for 45 minutes prior to fractography. However, this technique was not able to remove all corrosion products.

The distribution and arrangement of dislocations after fatigue cycling for cold rolled and for annealed materials of alloy 25 were examined by viewing thin films on a Phillips 400 transmission electron microscope (TEM) at an accelerating voltage of 120 KV. The TEM foils were obtained by jet polishing of electro-discharge cut circles using a 50% (by volume) phosphoric acid solution. This process was conducted at ambient temperature and under 100 mA current.

3. RESULTS AND DISCUSSION

3.1 Tensile Results

Comparing smooth and notched tensile data in Table 2.2, one can see the notch strengthening effects for annealed and aged materials. As mentioned in section 1.3.1, introducing a notch results in triaxial constraint which reduces the local plastic deformation at notch tip. It might be expected that this constraint would increase both yield strength and ultimate tensile strength of the material. But as seen in Table 2.2, an increase in the yield strength has been accompanied by no change or even a decrease in the tensile strength. The reason for this observation is that constraint of plastic deformation lowers the ductility and therefore, does not allow the material to take advantage of strain hardening leading to premature fracture. This argument is graphically shown in Figure 3.1 where stress-strain curves for smooth and notched specimens of annealed material are plotted. In the case of cold rolled material (alloy25-TDO4), as seen in Table 2.1, no considerable change was observed. However, one may attribute the slight decrease of yield strength to the notch weakening. As discussed in §1.3.1, notch weakening is expected when the material is brittle. Note that both notch weakening and strengthening phenomena can be better seen in more severe notches that apply higher stress concentrations. According to Peterson[31], K_t in these experiments was 2.73.

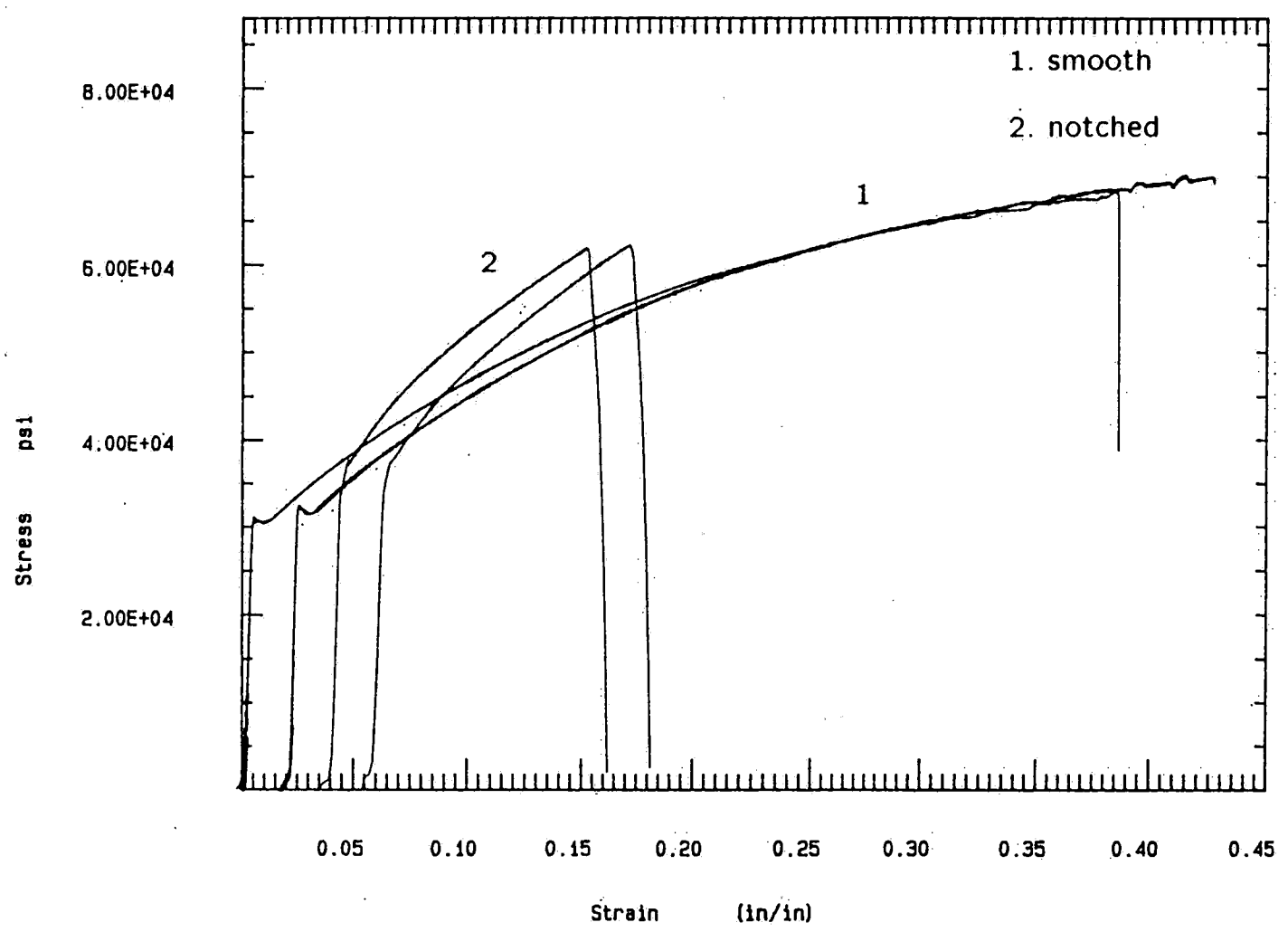

Figure 3.1. Smooth and notched tensile results for alloy 25 in the annealed condition.

3.2 Ambient Air Fatigue

3.2.1 Effects of Production Variables

The effect of a 7% tensile strain on the fatigue strength of alloy 10 in the cold rolled and aged condition is seen in Figure 3.2. A slight increase in fatigue strength of this material is due to an increase in the strength of the material after stretching.

Figures 3.3 and 3.4 show the effects of cold forming and heat treatment on the fatigue strength of alloy 25 in the absence and in the presence of notch, respectively. From these plots, one sees that the difference in fatigue strength of the various material conditions decrease with increasing cycles reaching a minimum at long lives. As shown in Figure 3.4, in the presence of notch and at high cycles, there is nearly no difference between high and low strength materials.

The smaller difference between fatigue strength of materials at high cycles than for low cycles, can also be explained by the change in flow strength experienced by the material during cycling. As discussed in section 1.2.1, depending upon the density and arrangement of dislocations present in the material, hardening or softening can be expected in fatigue cycling. According to Smith et al[27] cyclic hardening would be expected in the annealed material, whereas the rest of the materials should undergo softening and/or no significant change. The first phenomenon is clearly shown in Figure 3.5 where the stress-strain curve of alloy 25 in the annealed condition before and after fatigue cycling is presented. The particular specimen tested was one surving 2×10^6 cycles at σ_a= 25(ksi) without failure. As can be seen, cyclic hardening in the fatigued sample resulted in a 120% increase in the flow strength.

A clearer picture of the fatigue data for alloy 25 results from plotting the normalized stress rate ΔS/UTS as in Figures 3.6 and 3.7. On the normalized basis it is evident that annealed material is superior to cold rolled or cold rolled and aged for all cyclic lives and for both notched and unnotched specimens. An exception to this statement is the unnotched data for fatigue life at less than 10^4 cycles. In this case, Figure 3.6, the cyclic life is so short that fatigue tests with a stress ratio of 0.1 are really not too different from monotonic tensile tests. On the other hand, in the presence of a notch, Figure 3.7, the superiority of annealed material at short life probably reflects a greater capacity for blunting of the notch in the lower strength materials. For lives of 10^6 cycles, cyclic hardening is probably responsible for the superiority of annealed material as illustrated in Figure 3.5.

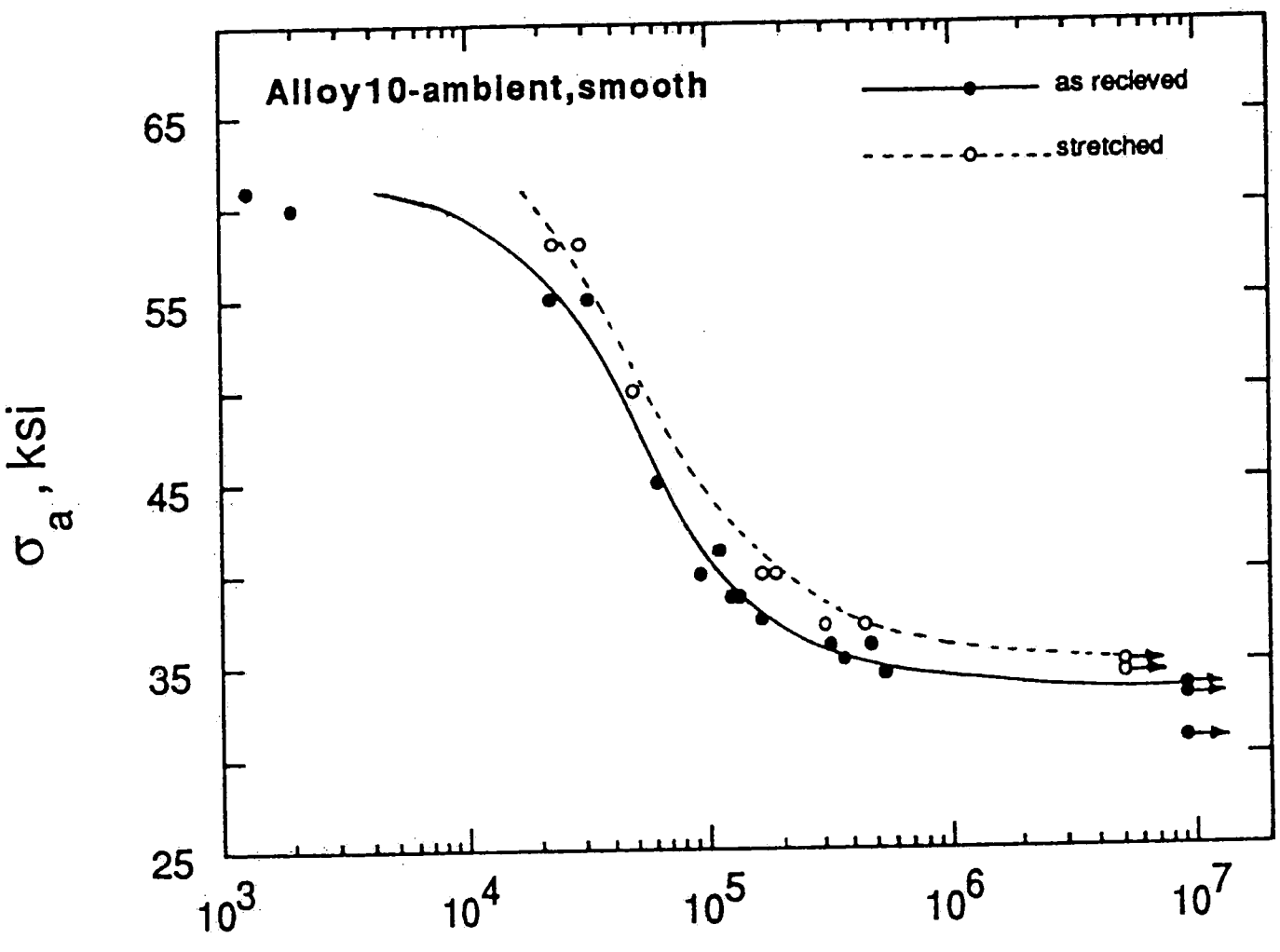

Figure 3.2. Effect of 7% tensile strain on the fatigue strength of alloy 10 in the cold rolled and aged condition.

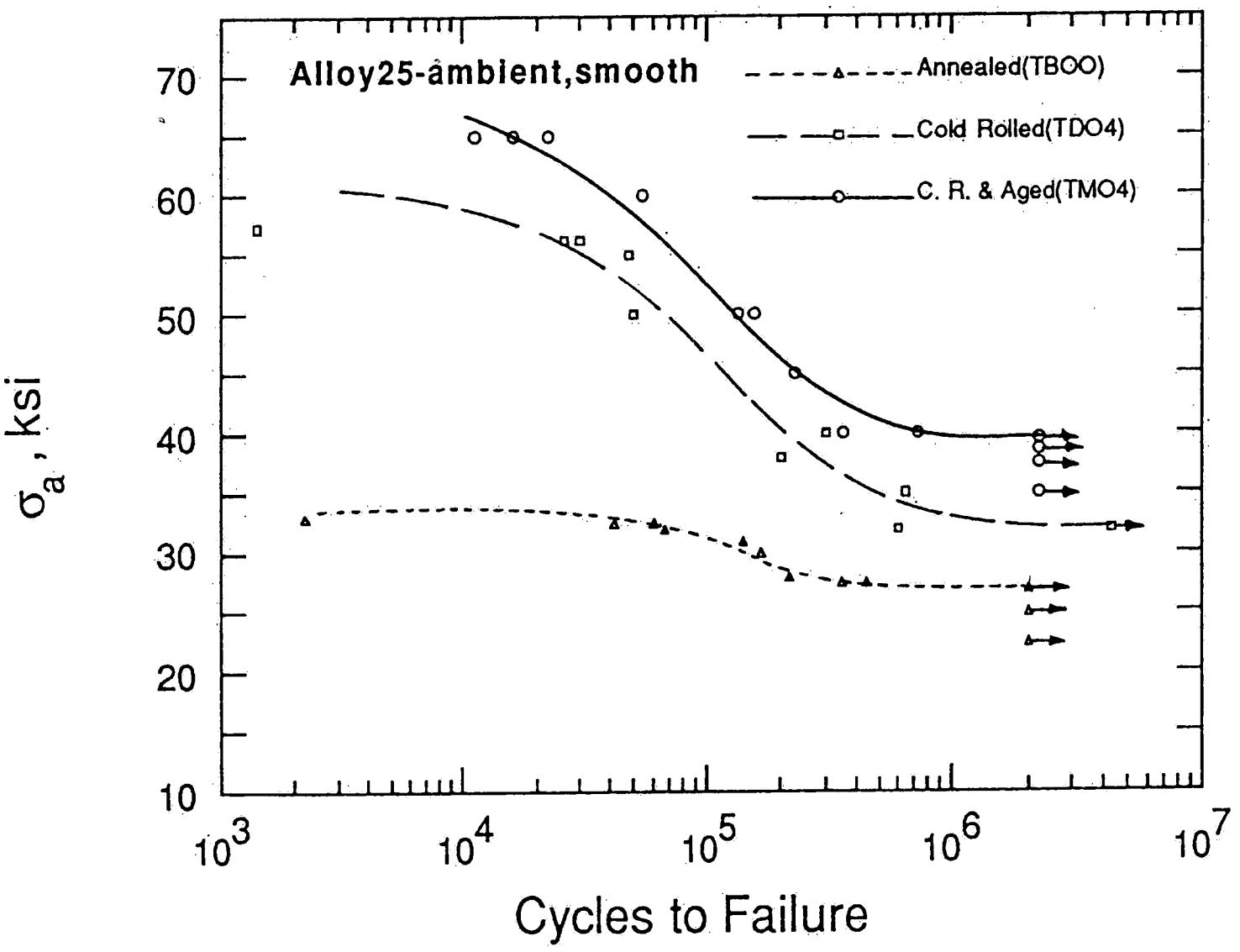

Figure 3.3. Effects of cold forming and heat treatment on the fatigue strength of alloy 25 in the absence of a notch.

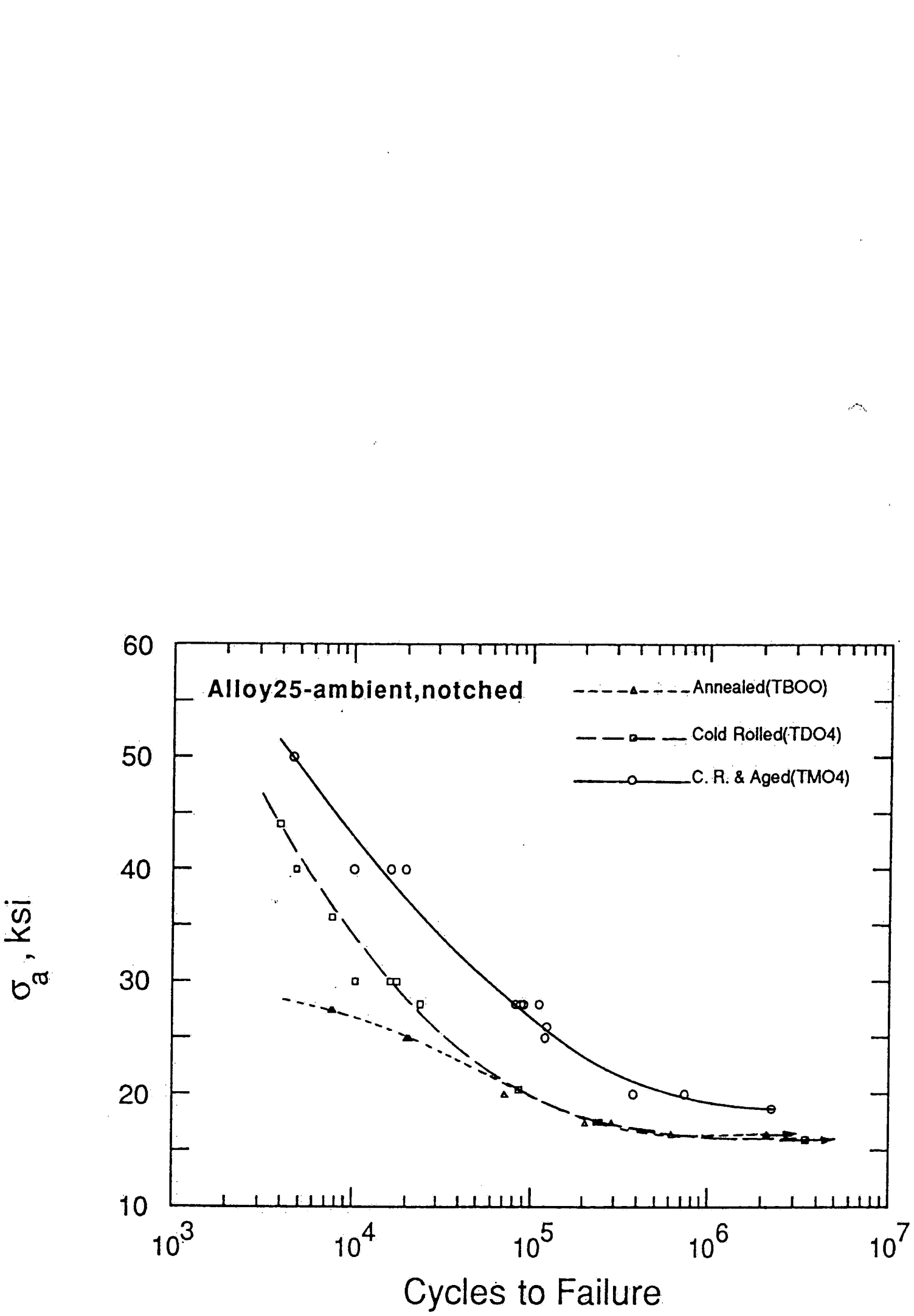

Figure 3.4. Effects of cold forming and heat treatment on fatigue strength of alloy 25 in the presence of a notch.

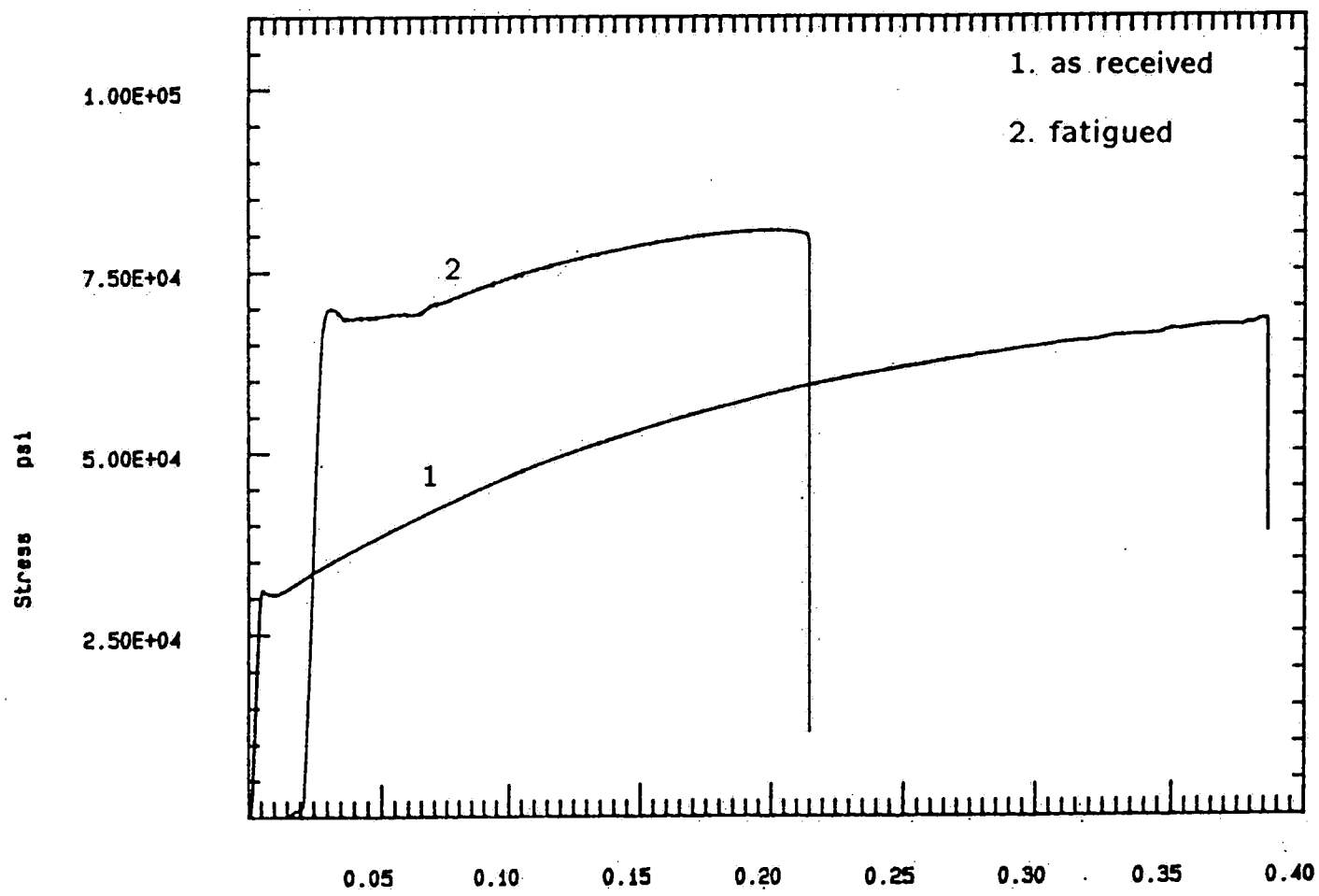

Figure 3.5. Cyclic hardening in annealed Be-Cu after 2×10^6 cycles at σ_a=25(ksi) resulted in 120% increase in flow strength.

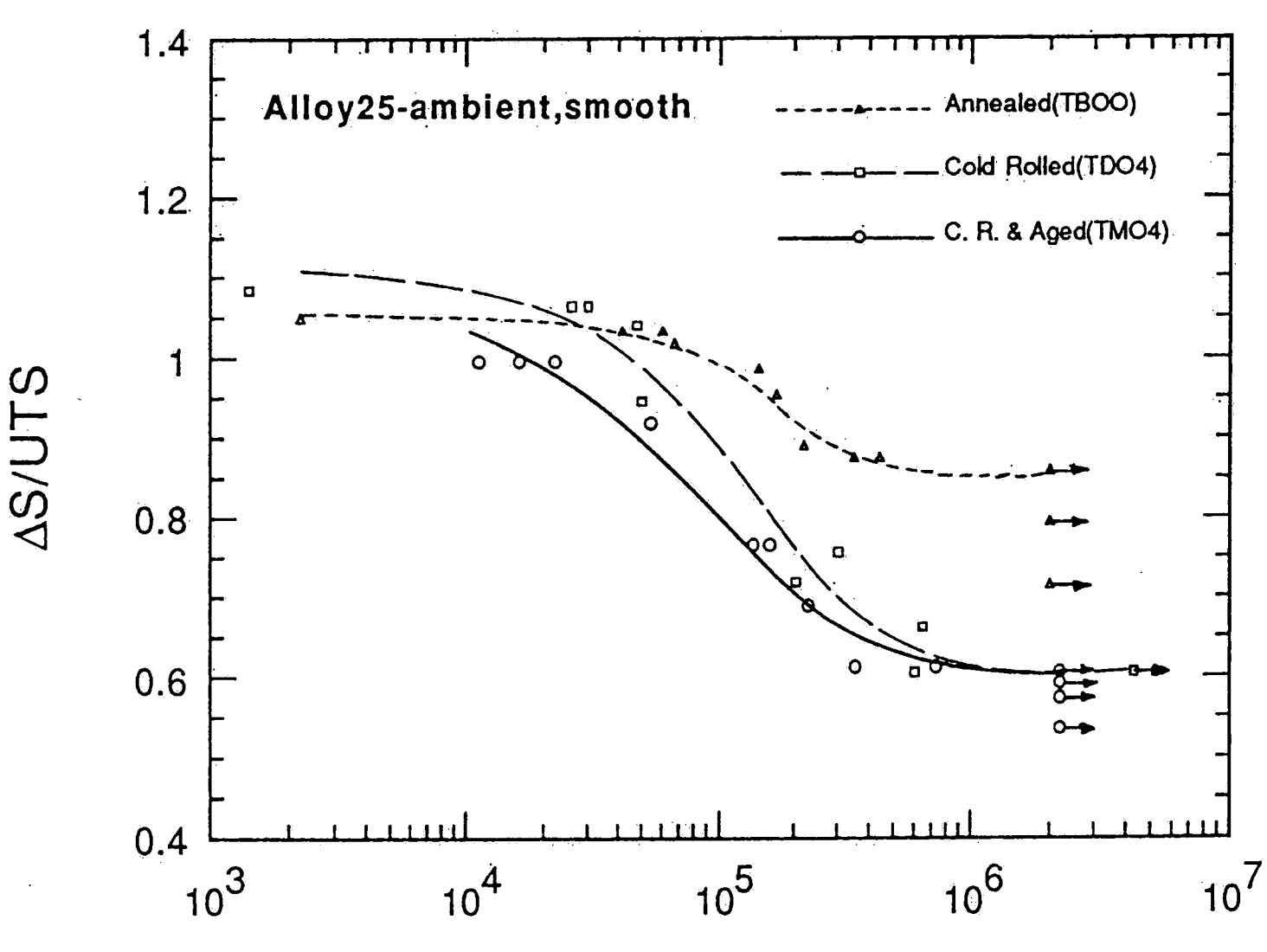

Figure 3.6. Effects of cold forming and heat treatment on fatigue strength of alloy 25 in the absence of a notch normalized by tensile strength.

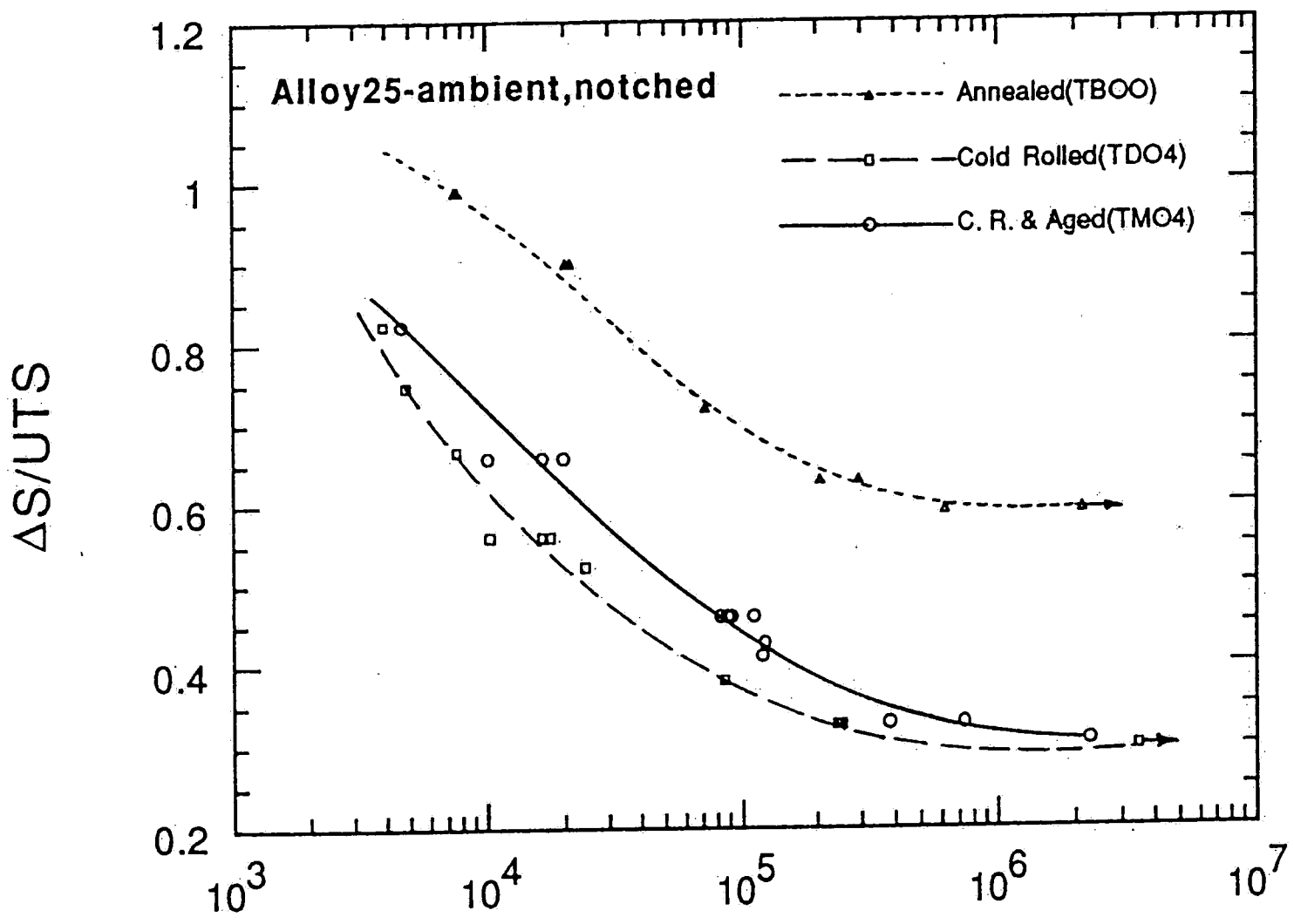

Figure 3.7. Effects of cold forming and heat treatment on fatigue strength of alloy 25 in the presence of a notch normalized by tensile strength.

As discussed in section 1.2.1, hardening or softening in fatigue cycling depends on the density of dislocations prior to fatigue and also on their rearrangement during fatigue. This concept was confirmed by transmission electron microscopy of fatigued samples of alloy 25 in the annealed and cold rolled conditions. Figure 3.8 shows the concentration of dislocation networks inside the grains in annealed material. However, in the cold rolled specimen, dislocations were found to be much more concentrated at grain boundaries, Figure 3.9. This observation is consistent with that of Awatani et al[28] and indicates that fatigue reversals have caused softening in cold rolled material through the concentration of dislocations close to grain boundaries. Hardening, on the other hand, has occured in fatigue cycling of the relatively low-dislocation-density material by rearranging of dislocations inside the grains.

Finally, refering again to Figure 3.5, suggests the possible influence of strain aging on cyclic hardening of annealed Be-Cu alloy. Working on yielding phenomenon in copper alloys, Jones and Phillips[42] reported no initial yield point in solution treated and in aged Be-Cu. However, they found that this phenomenon could be produced by suitable cold working and strain aging. In such a treatment, Cottrell atmospheres form around the dislocations by vacancy assisted diffusion of beryllium atoms. They argued that continuing the aging treatment caused precipitation of solute atoms along the dislocation lines and consequently results in a marked increase in the yield strength. Comparing Jones and Phillips[42]results with the observation of yielding phenomenon in this study, one can say that fatigue cycling has provided suitable conditions for dislocation locking, similar to that of combination of cold working and heat treatment.

Fatigue induced strain aging has been also reported in low-carbon steel[43,44]. In these studies, the observation of a fatigue limit is attributed to strain aging. It is also claimed that strain aging, during cycling, increases the constraints imposed on regions of plastic deformation results in strengthening of the material, especially in stage I of crack growth.

While strain aging was not a major part of this study, it is likely that the interaction between dislocations, or their network, and locking agents in fatigue of annealed Be-Cu plays an important role in cyclic hardening of this material. In other words, both the dislocation arrangement and strain aging are responsible for cyclic hardening of annealed material.

Figure 3.8. TEM micrograph of annealed Be-Cu after 2×10^6 fatigue cycles showing the distribution of dislocations inside grains. The arrow indicates the grain boundary.

INTENTIONAL SECOND EXPOSURE

Figure 3.8. TEM micrograph of annealed Be-Cu after 2×10^6 fatigue cycles showing the distribution of dislocations inside grains. The arrow indicates the grain boundary.

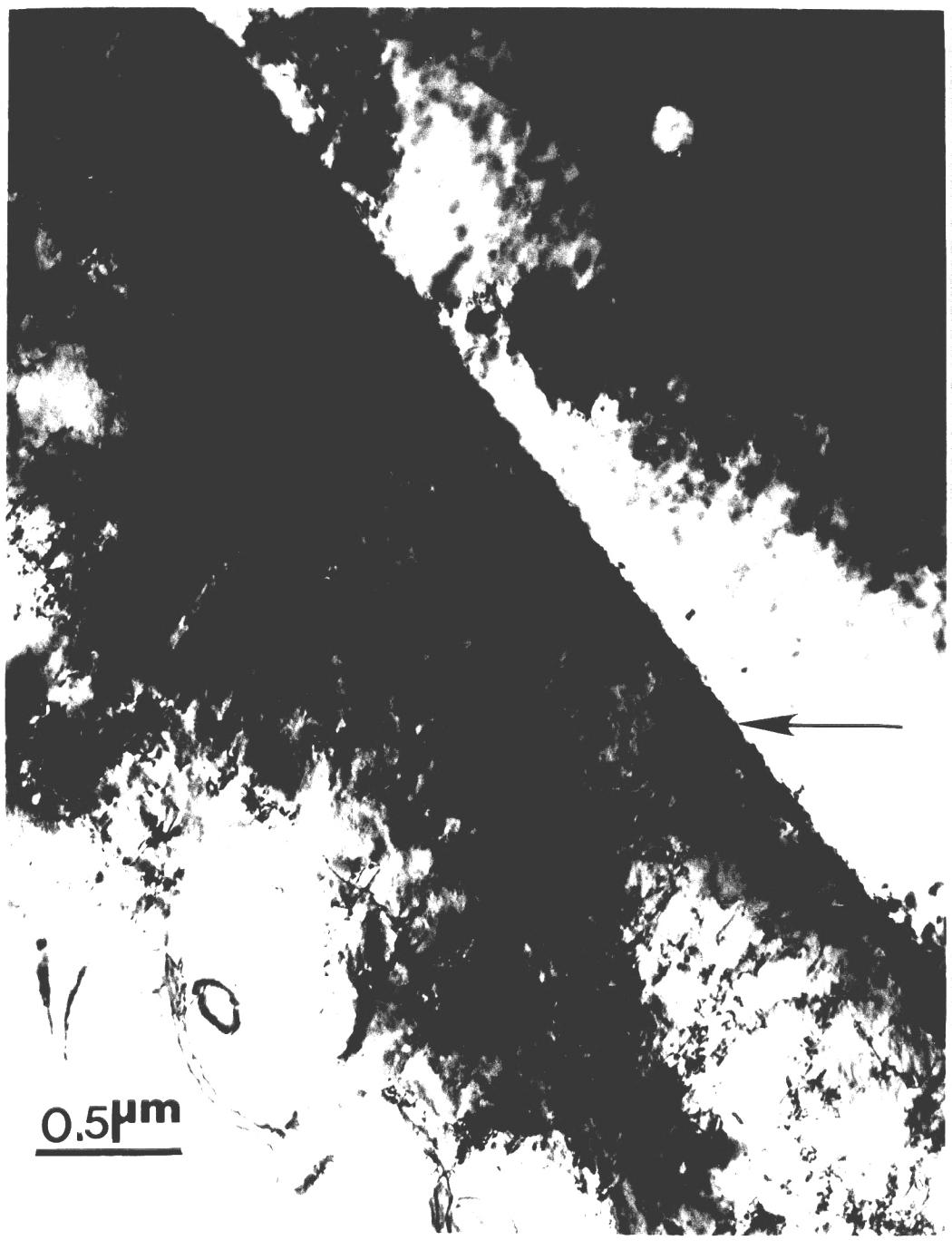

Figure 3.9. TEM micrograph of cold rolled Be-Cu after 4×10^6 fatigue cycles revealing the concentration of dislocations at, or in regions close to, grain boundary. The arrow shows the grain boundary.

Figure 3.9. TEM micrograph of cold rolled Be-Cu after 4×10^6 fatigue cycles revealing the concentration of dislocations at, or in regions close to, grain boundary. The arrow shows the grain boundary.

3.2.2 Notch Effects

Figures 3.10–3.13 show the notch effect on fatigue strength of four materials tested. As expected, for a given life, the notched sample tolerates much less stress* than that of the smooth one. The notch effect is usually described by the fatigue notch factor (K_f) or notch sensitivity factor (q). Variations of K_f and q for different conditions of alloy 25 versus number of cycles to failure are shown in Figures 3.14 and 3.16, respectively. As seen in these Figures, both K_f and q increase as the number of cycles to failure increases. This observation confirms that the more deleterious effect of notches is at high cycles, or better, at low loads. The reason for this more harmful effect, as dicussed before, relates to less plastic deformation at the lower loads.

Another feature of Figure 3.14 is the dependence of K_f on the strength of the material. This concept is shown in a different way in Figure 3.15 where K_f is plotted versus ultimate tensile strength for different fatigue lives of alloy 25. According to this Figure, the general idea of increasing K_f with increasing strength of material is true for tensile strength in the range of 70 to 115 ksi. Beyond 115 ksi, K_f is nearly constant. As seen here, the cold rolled material that has relatively high strength but very low ductility, has the highest fatigue notch factor. This observation, again, illustrates the blunting effect of plastic deformation at notch tip. The conclusion here is that any treatment which results in more brittle behavior, in a given alloy, increases the deleterious effect of notches.

The given equation for K_f-K_t relation:

$$K_f = 1 + \frac{K_t - 1}{1 + \sqrt{A/\rho}} \qquad (1)$$

was examined using measured K_f values in this study. No dependence of the constant A in this equation on grain size was found which is not consistent with what Collins[34] reported. Between ultimate tensile and yield strength, the latter showed a better relationship with A. The dependence of A on yield strength in Be-Cu alloys tested and some low-carbon steels[45] are shown in Figure 3.17. As seen, the constant A increases as the yield strength decreases. A in equation (1) has the dimension of length. This means that for a given notch root radius, K_f and K_t are related through a distance parameter and this distance parameter is proportional to the inverse of the yield stress.

---

* In notched samples, the stress is the net nominal stress applied to the specimen.

This finding is similar to what Azimi[46] has observed. He found that in notched specimens, the maximum damage occurs not at the notch tip, but at a distance in front of it and that this distance is proportional to the inverse of the yield strength. Comparing two sets of results, it can be concluded that K_f is equal to the magnitude of K_t at a distance in front of the notch tip. This distance which depends on the ability of the material to blunt the crack, can be explained by the yield strength and should be proportional to A in equation 1.

In spite of its benefits, equation 1 for the K_f-K_t relationship still has some problems. This equation does not account for the effect of mean stress. Moreover, this equation shows a linear relationship between K_f and K_t, while it is not the case. Note that after a critical K_t, increasing stress concentration has no more effect on K_f[33]. These problems suggest caution in using of the equation 1. However, this equation can be employed to have an idea about K_f in many circumstances.

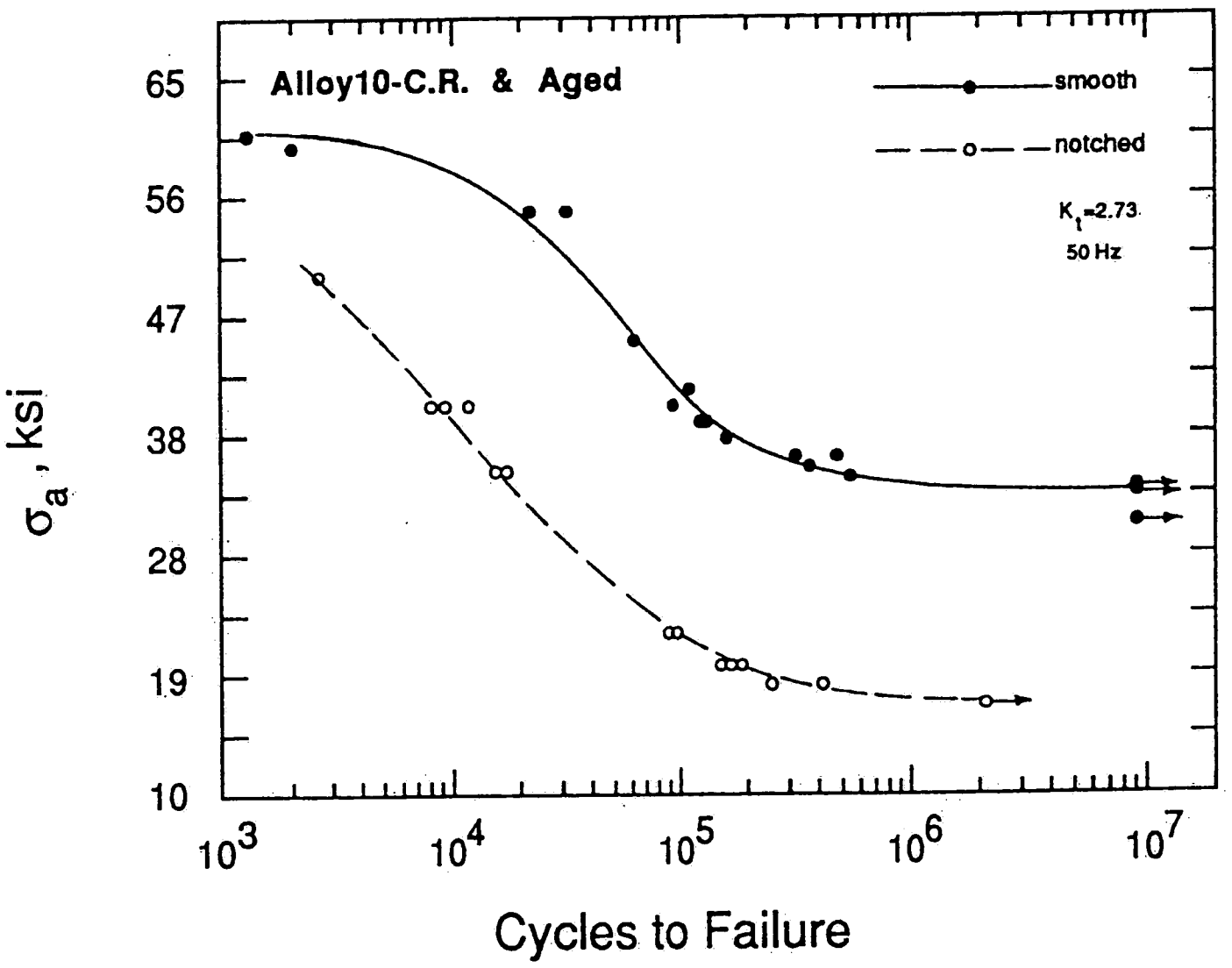

Figure 3.10. Notch effect on the ambient air fatigue strength of alloy 10 in the cold rolled and aged condition.

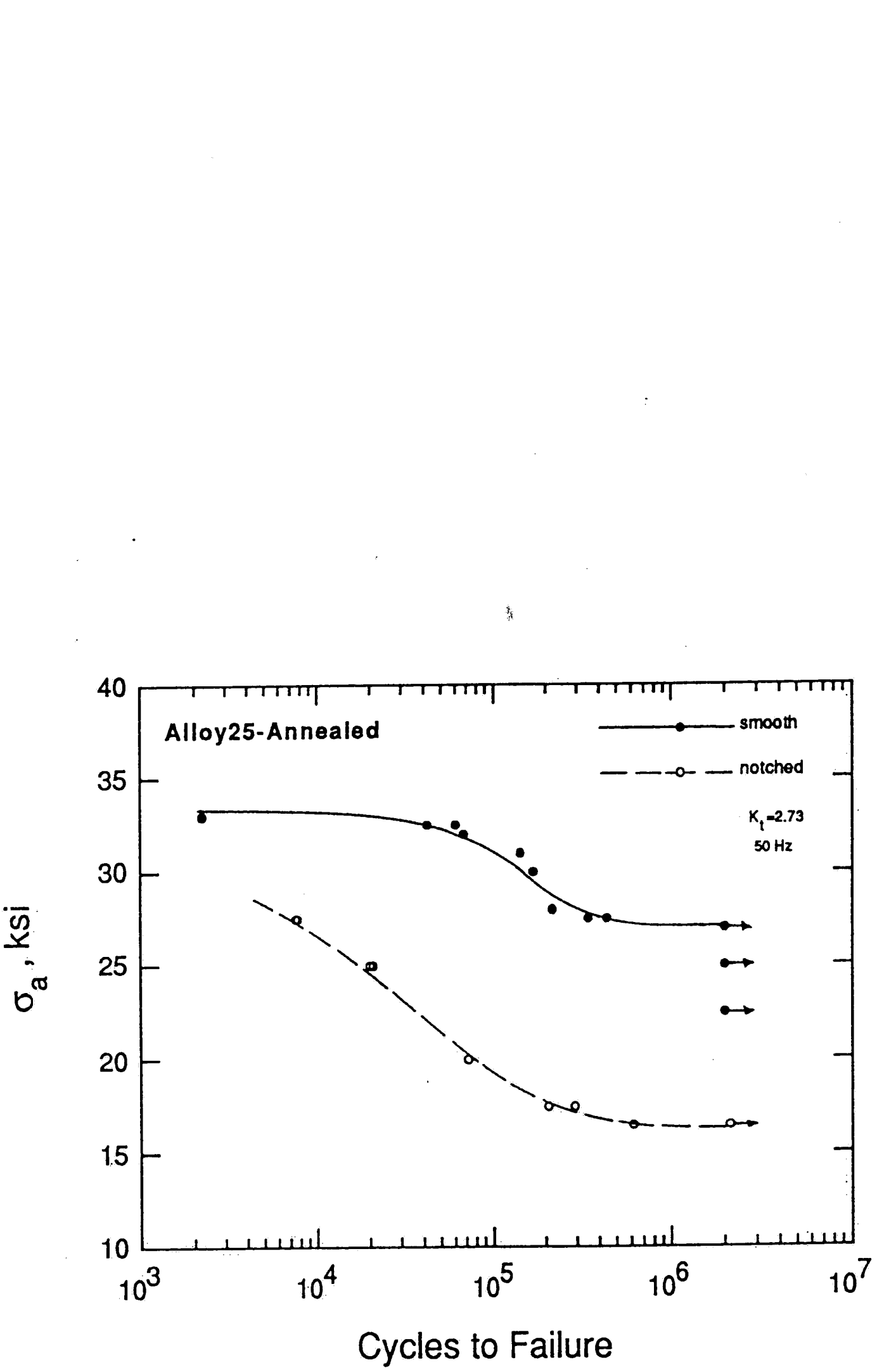

Figure 3.11. Notch effect on the ambient air fatigue strength of alloy 25 in the annealed condition.

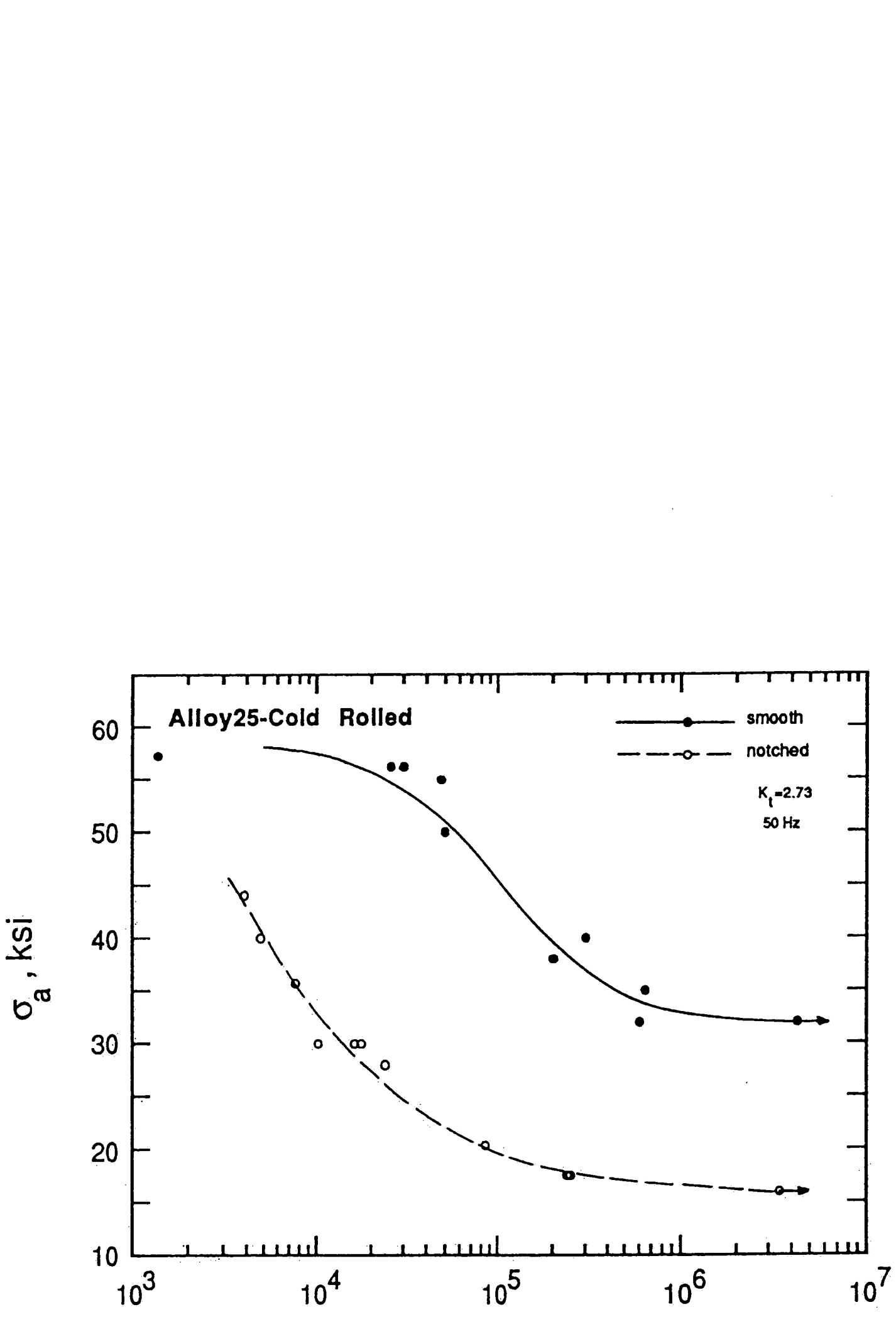

Figure 3.12. Notch effect on the ambient air fatigue strength of alloy 25 in the cold rolled condition.

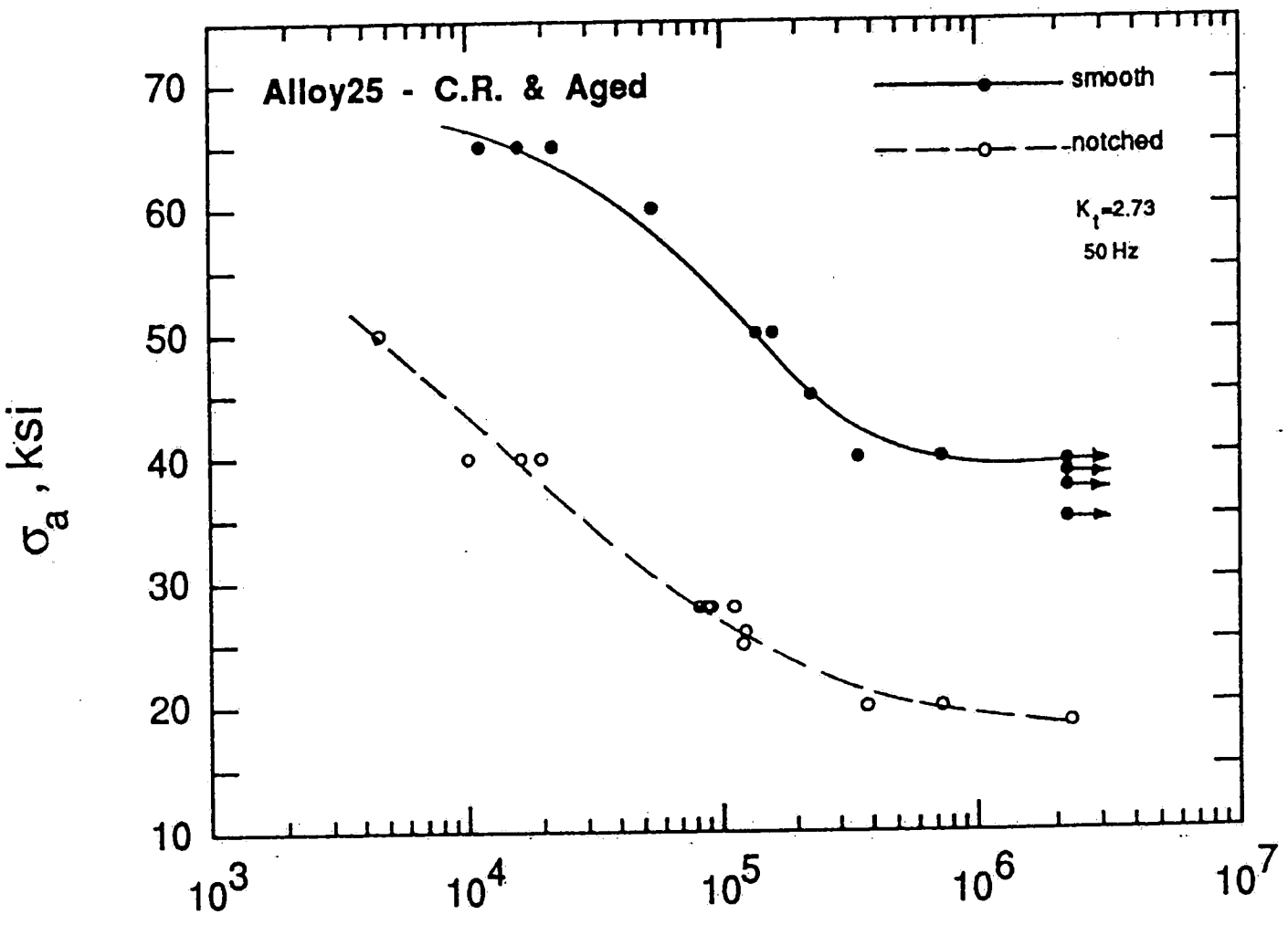

Figure 3.13. Notch effect on the ambient air fatigue strength of alloy 25 in the cold rolled and aged condition.

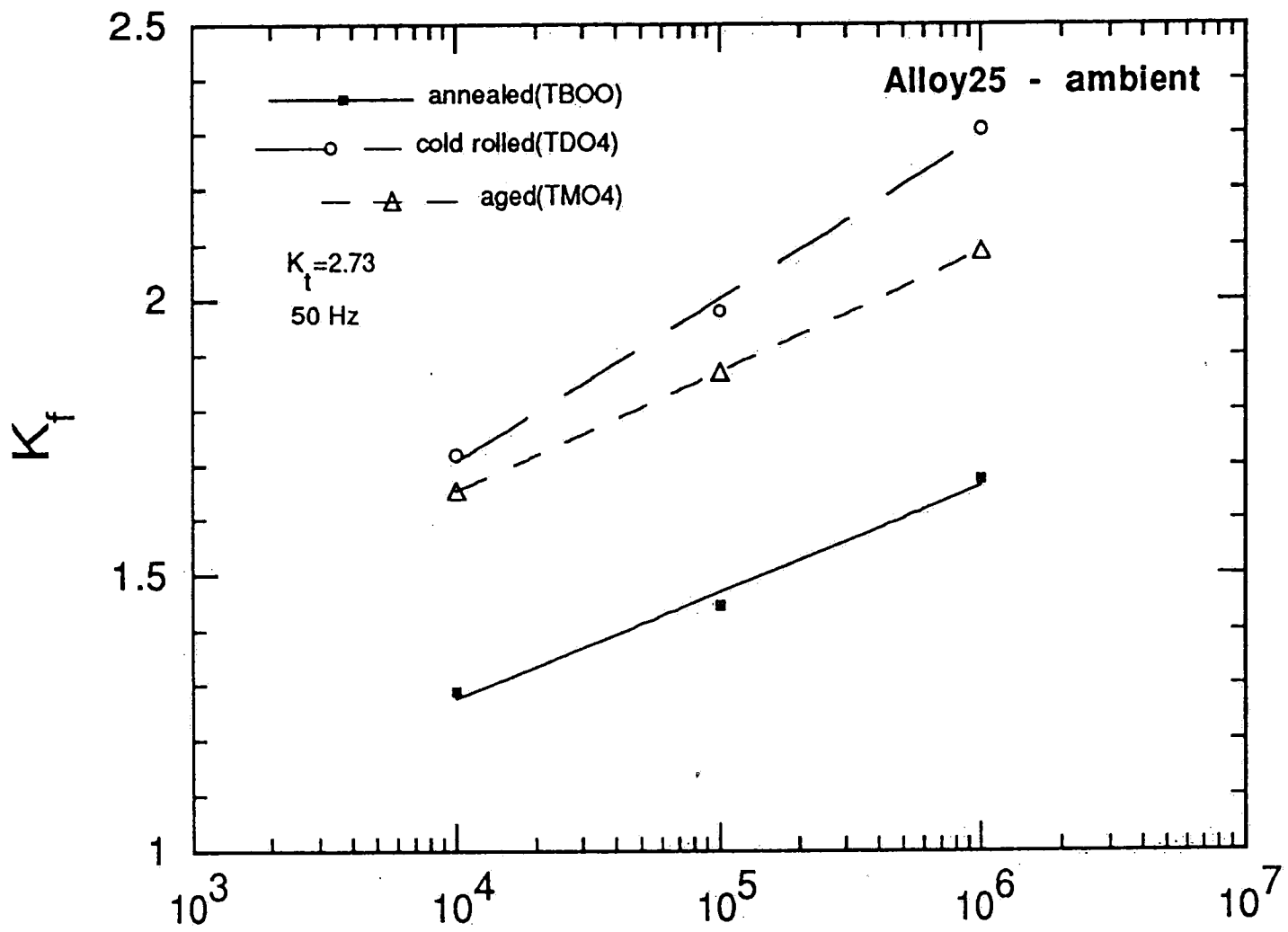

Figure 3.14. Effect of treatment condition on the fatigue notch factor (K_f) of alloy 25 for different fatigue life in ambient air.

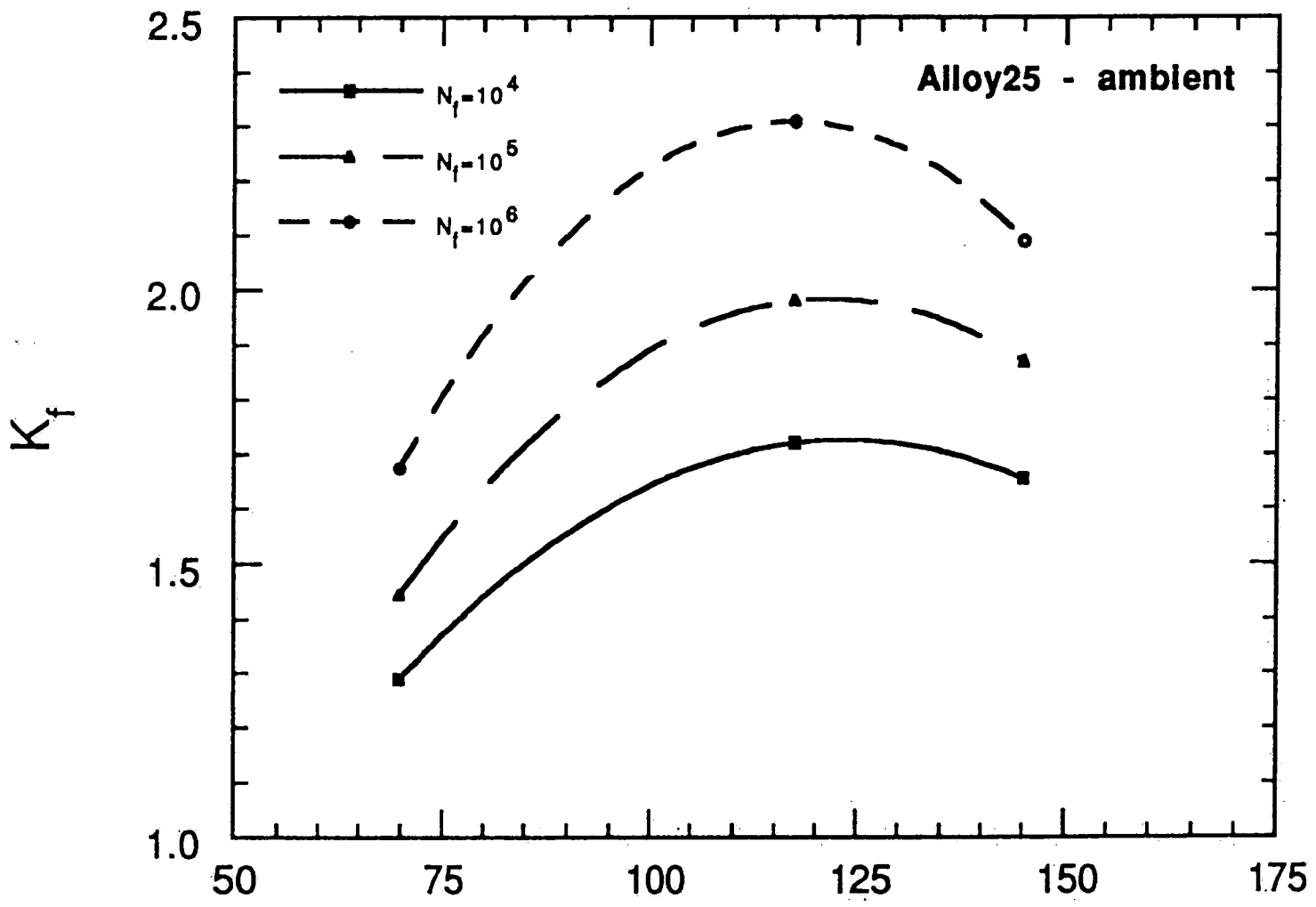

Figure 3.15. Variation of K_f in alloy 25 as a function of ultimate tensile strength.

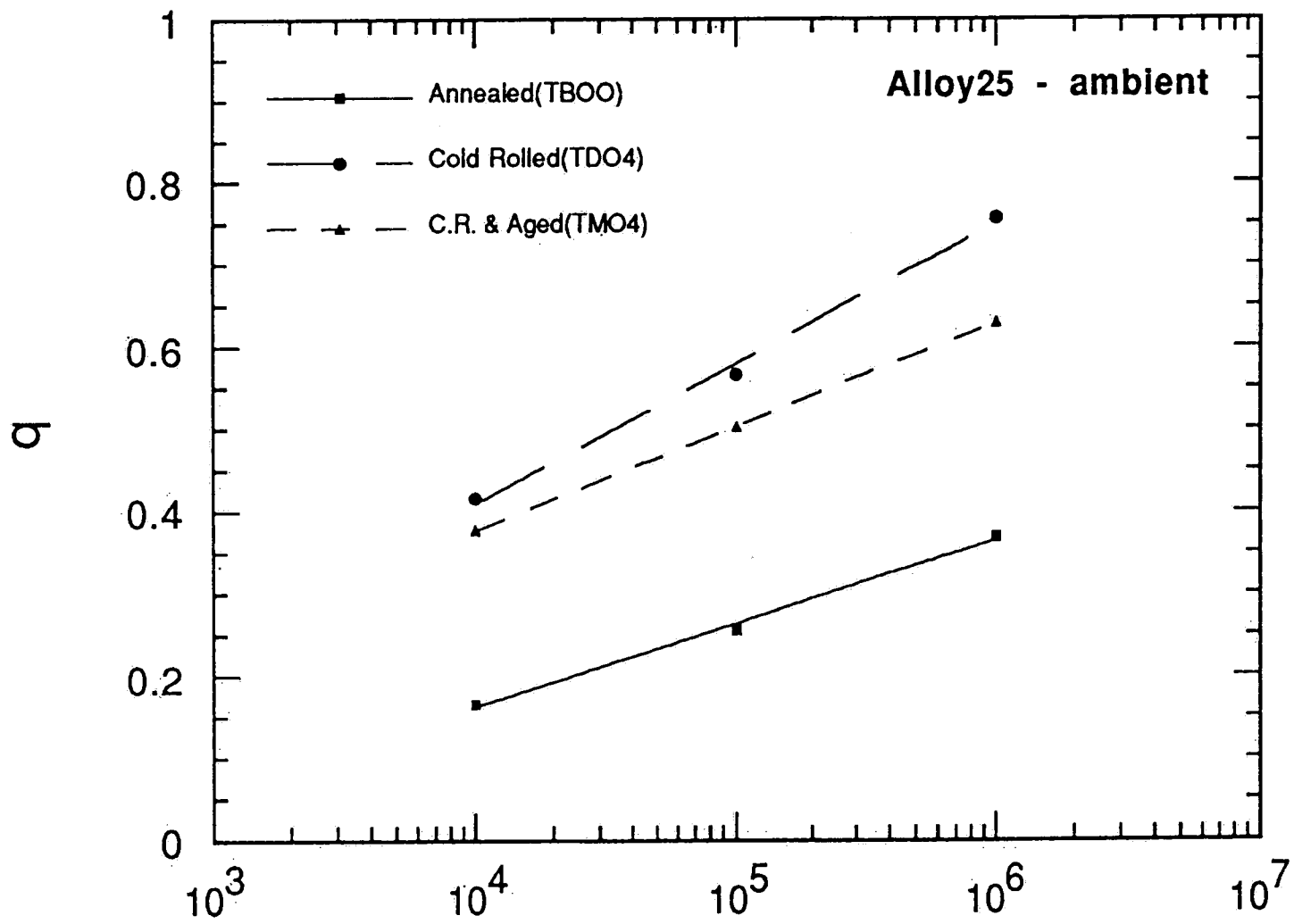

Figure 3.16. Effect of treatment condition on notch sensitivity factor (q) of alloy 25 for different fatigue lives.

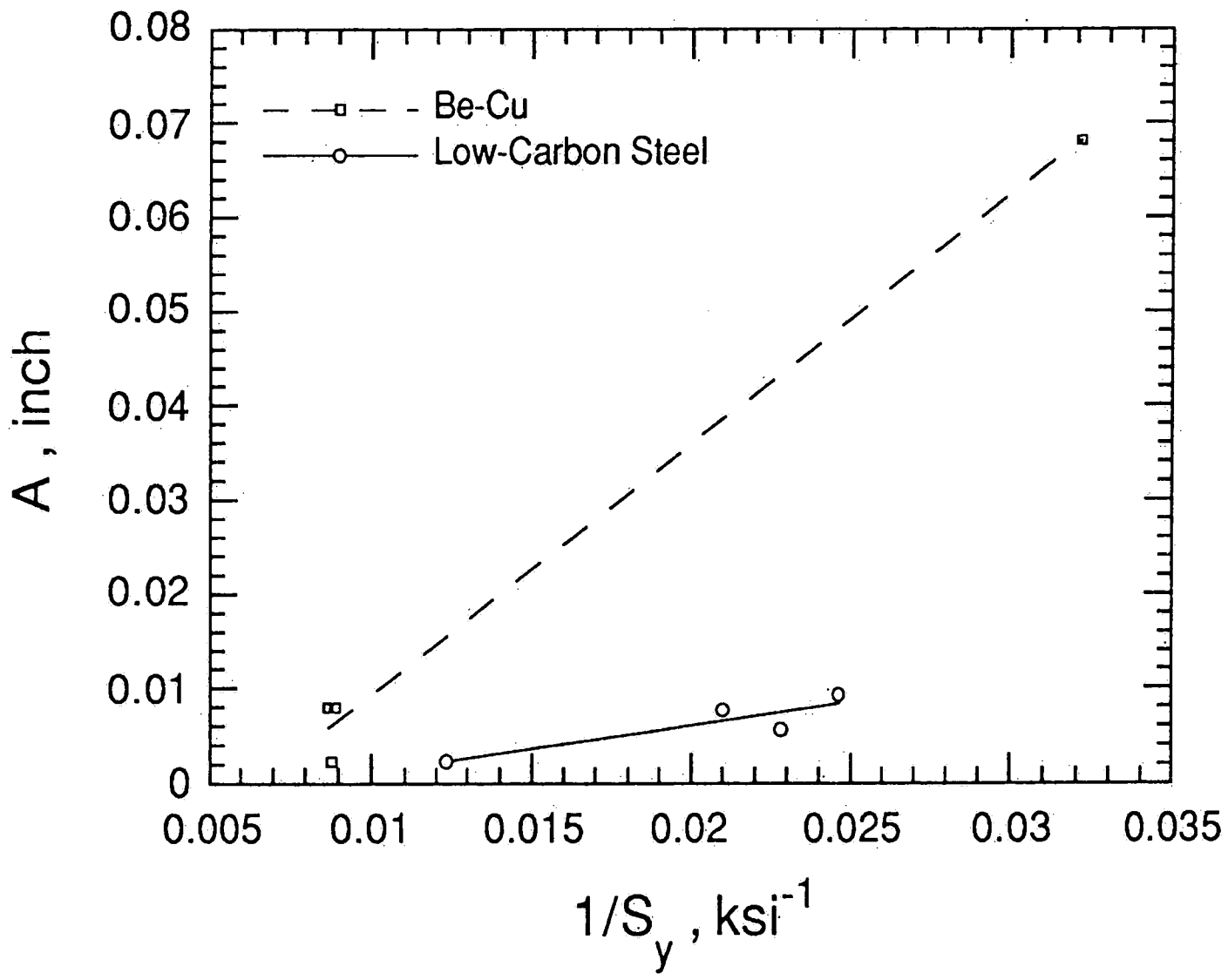

Figure 3.17. Variation of the constant A in the K_f-K_t relation, equation 1, as a function of the yield strength for some low-carbon steels[45] and Be-Cu alloys tested.

3.3 Corrosion Fatigue

The highest and lowest strength materials, alloy 25TBOO and 25TMO4, respectively, were selected for testing in brine. Figures 3.18 and 3.19 show the effect of aqueous environment on the fatigue strength of annealed and cold rolled and aged materials, respectively.

3.3.1 Smooth Results

The environmental effect is greater at high cycles than that of low cycles for both aged and annealed materials. This is due to the time dependent characteristics of corrosion. Aqueous medium lowered fatigue strength of solution annealed Be-Cu by about 10% for a life of 3×10^5 cycles, while the same environment at the same lifetime decreased the fatigue strength of cold rolled and aged material by more than 37%. This difference is attributed to the difference in strength of the two materials. As discussed in section 1.2, the high strength material has more regions of high energy which are prone to environmental attack than that of the annealed material. These regions of high energy include the matrix/precipitate interface and the regions of high concentration of dislocations.

The effect of frequency on corrosion fatigue is seen by comparing these results with those of other investigations on Be-Cu. For example, Richards[6] reported no difference in corrosion fatigue strength between solutionized and aged Be-Cu, while his materials were tested at 20 Hz. Also, he did not see any appreciable decrease in fatigue strength of both materials in salt water as compared to that of air fatigue. Decreasing the cyclic frequency from 20 to 1 Hz, increases the exposure time and may be responsible for the difference between current findings and those of Richards[6]. Considering the point that most real cases involve low frequency conditions, it can be stated that high frequency corrosion fatigue tests are not very useful in predicting service performance.

The effect of oxygen present in the environment is another important feature of the corrosion fatigue response. The corrosion chambers used in this study had openings to allow aeration of the environment. Two tests using chambers without any opening were performed on aged material. The results which are not reported in

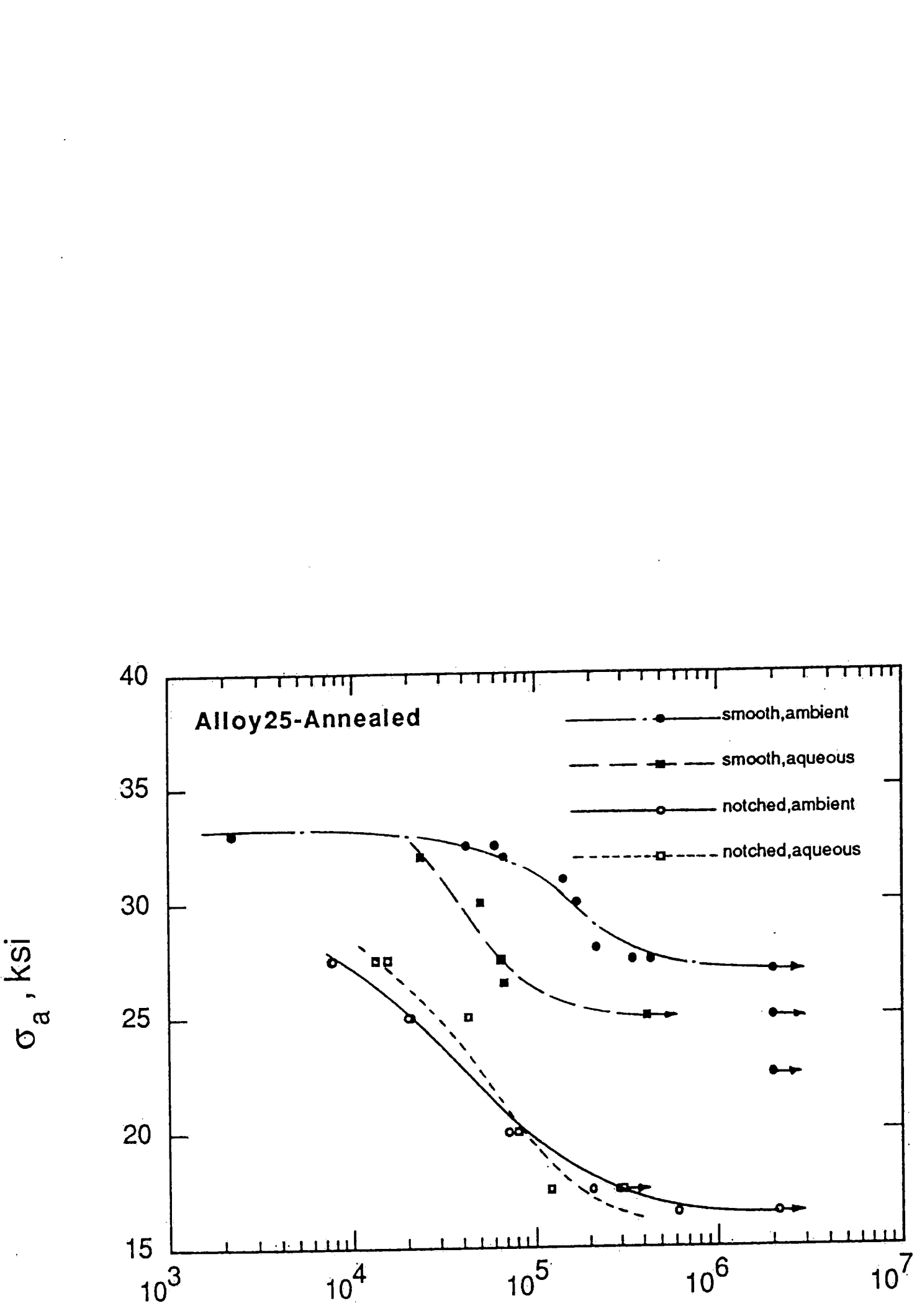

Figure 3.18. Effect of aqueous environment on fatigue strength of alloy 25 in the annealed condition.

Figure 3.19. Effect of aqueous environment on fatigue strength of alloy 25 in the aged condition.

Figure 3.19, revealed about a 60% increase in fatigue life in comparison with tests using open chambers at the same stress level. Considering the fact that these two tests were not conducted in completely deaerated condition, it is possible that there is no environmental effect on fatigue strength of Be-Cu in deaerated brine. This is similar to what Mehdizadeh et al[23] observed in their study on corrosion fatigue of some low carbon steels.

3.3.2 Notched Results

In contrast to what was observed in corrosion fatigue testing of smooth samples, in the presence of notch in both annealed and aged materials there was almost no environmental effect (Figures 3.18 and 3.19). The reason for this paradoxical result is the effect of the notch in reducing the initiation component of life due to the stress concentration and because the major part of fatigue life in these fine gage strips is consumed in crack initiation*. However, it is not clear why there is no effect for notched specimens since it can be argued that at the lower frequency used in this study, notched specimens should not be free of corrosion damage.

Scanning electron microscopy of fracture surface of air-fatigued materials revealed that in both smooth and notched samples of aged material, fatigue crack initiated on slip planes and followed the crystallographic directions (Figure 3.20). In smooth samples this texture changed very soon to a dimple-like mode (Figure 3.21). The fatigue crack then propagated through the entire surface in this mode, until the fast fracture region. But, in notched specimens, the cleavage-like fatigue fracture observed during early propagation did not change until the fast fracture.

Changing fracture mode from a ductile manner, i.e. dimples, in smooth samples to a brittle cleavage-like in notched specimens is consistent with the constraint effect of the notch discussed before. Note that in the case of notched samples, fatigue crack propagated less than 0.04 inch from the notch tip prior to the fast fracture.

---

* For most instances, it was impossible to stop cycling of a sample with a crack in it.

Figure 3.20. SEM fractograph of alloy 25 in the aged condition showing the transcrystalline fracture along spesific crystallographic planes in initiation site.

Figure 3.20. SEM fractograph of alloy 25 in the aged condition showing the transcrystalline fracture along spesific crystallographic planes in initiation site.

Figure 3.21. SEM fractograph of alloy 25 in the aged condition indicating the dimple-like fracture crack growth.

INTENTIONAL SECOND EXPOSURE

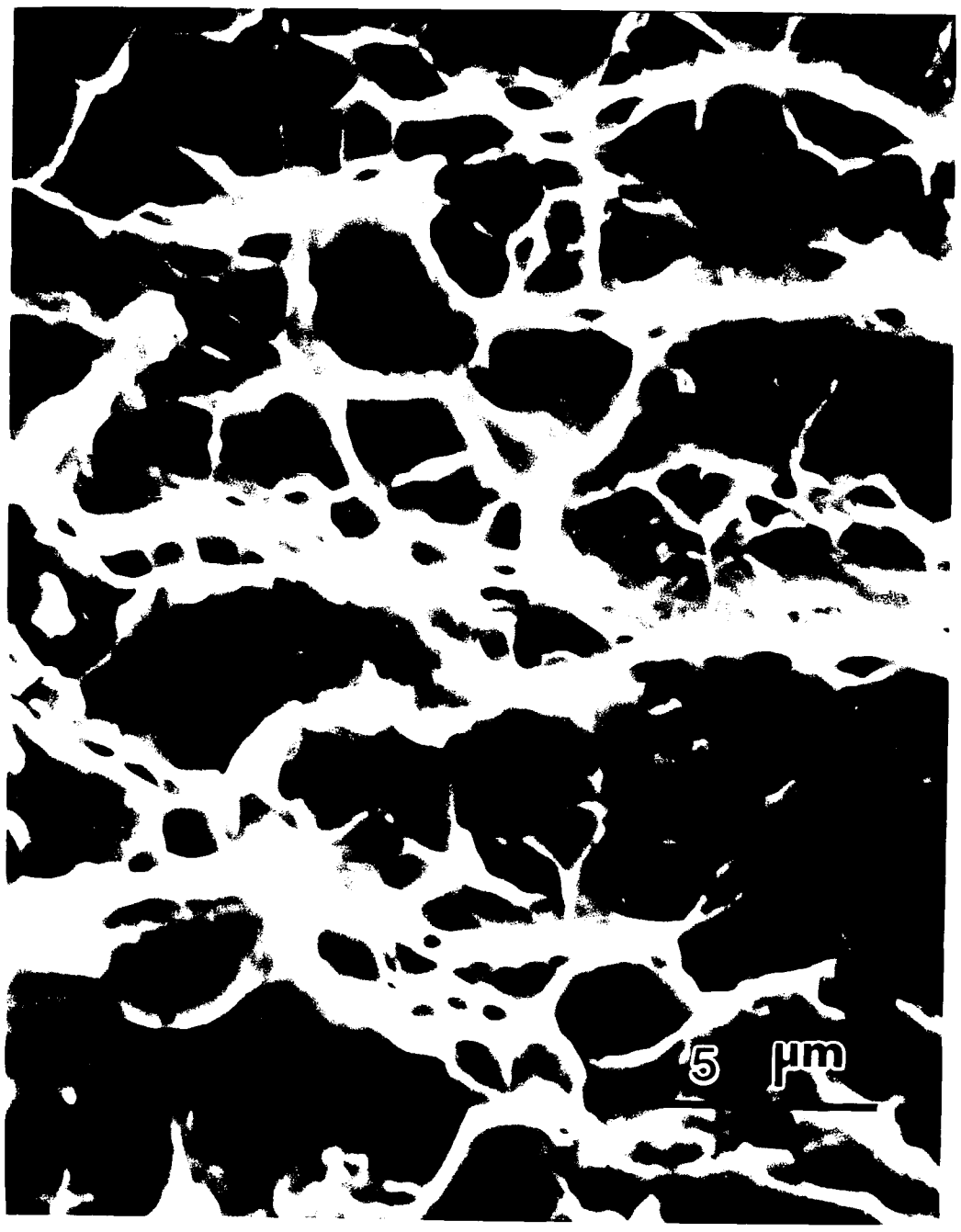

Figure 3.21. SEM fractograph of alloy 25 in the aged condition indicating the dimple-like fracture crack growth.

In annealed material no change in fracture mode was observed by the introduction of notch. In both smooth and notched samples, crack started at slip lines in a very ductile manner (Figure 3.22). Broek[47] argued that observation of this fracture surface represents the local blunting of cracks formed at slip lines, which is in agreement with very high ductility of this material. The irregular nature of slip lines distinguishes this texture from the fatigue striations that appeared later in both smooth and notched specimens (Figure 3.23).

No significant change was found in fractue surface of both annealed and aged materials when they were exposed to the salt water. However, secondary cracks, growing perpendicular to the direction of crack growth, were deepened and were much more visible in aqueous environment. Striations observed in annealed material were almost flat and more difficult to detect in aqueous environment. In all cases studied, the cracks followed a transgranular path and did not change in brine which is in contrast to what was reported for pure copper[13,30] and CuNiCr[21].

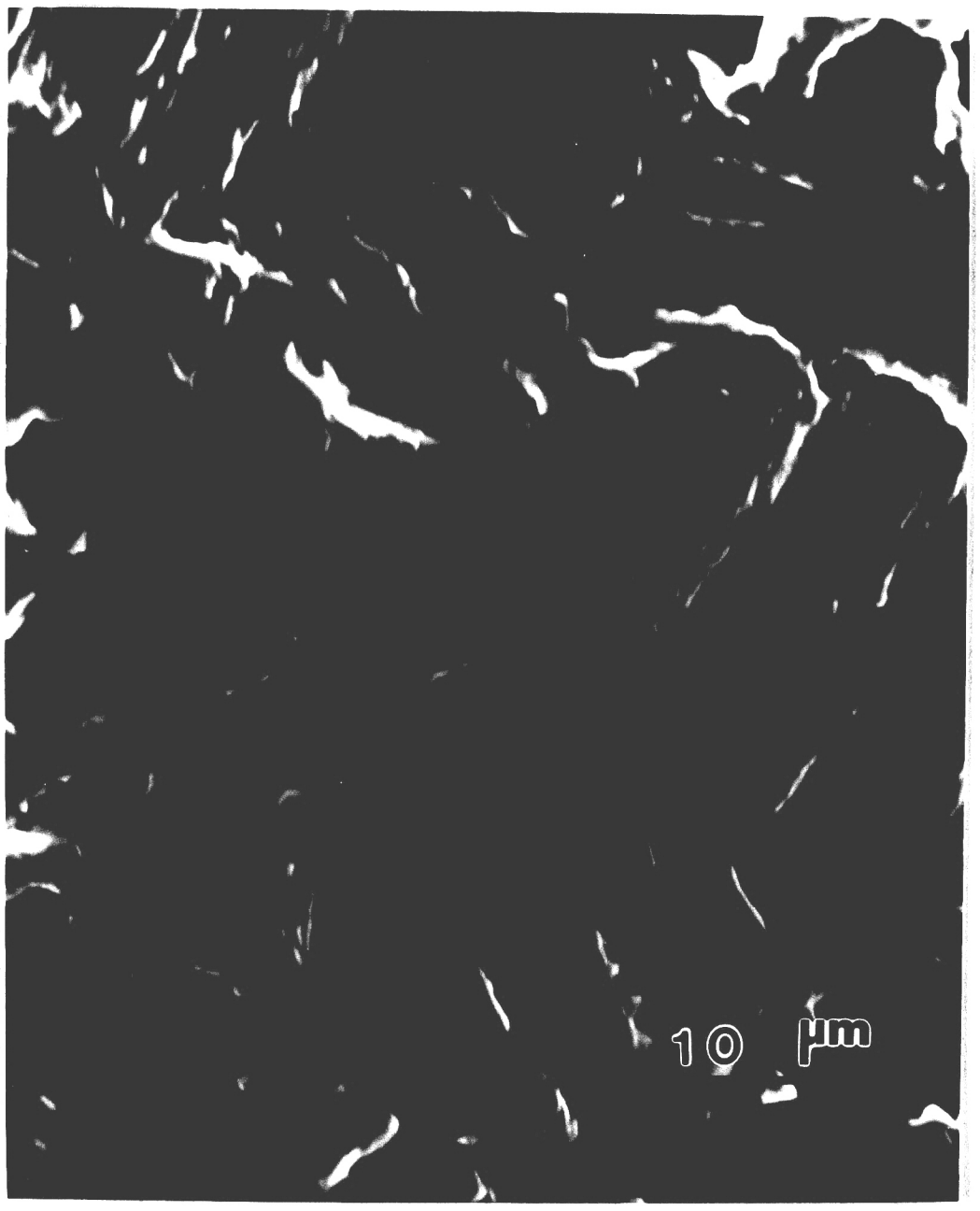

Figure 3.22. SEM fractograph of alloy 25 in the annealed condition showing crack initiation at slip lines which is associated with local blunting.

INTENTIONAL SECOND EXPOSURE

Figure 3.22. SEM fractograph of alloy 25 in the annealed condition showing crack initiation at slip lines which is associated with local blunting.

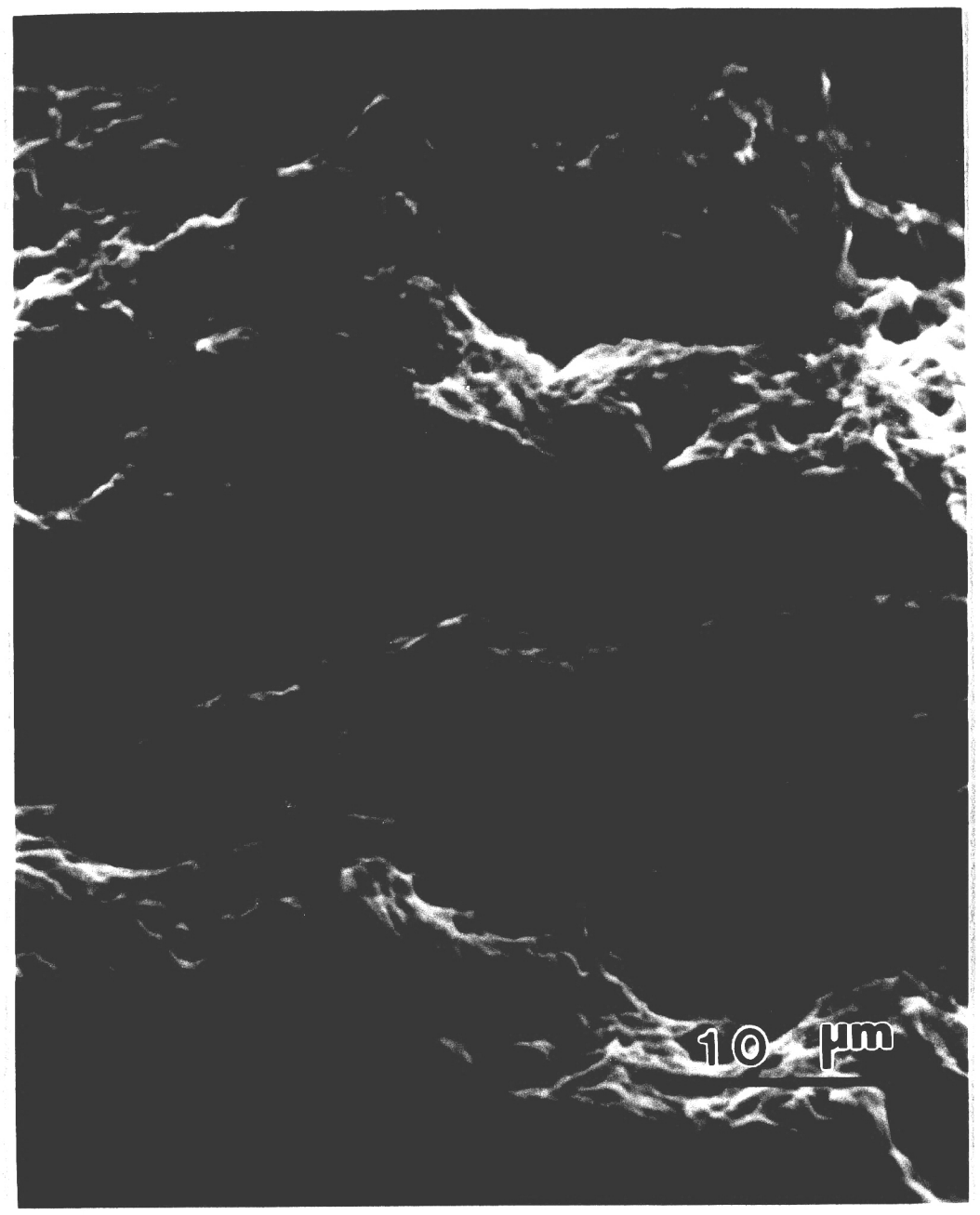

Figure 3.23. SEM fractograph of alloy 25 in the annealed condition showing fatigue striations along with high plastic deformation. The arrow indicate the crack growth direction.

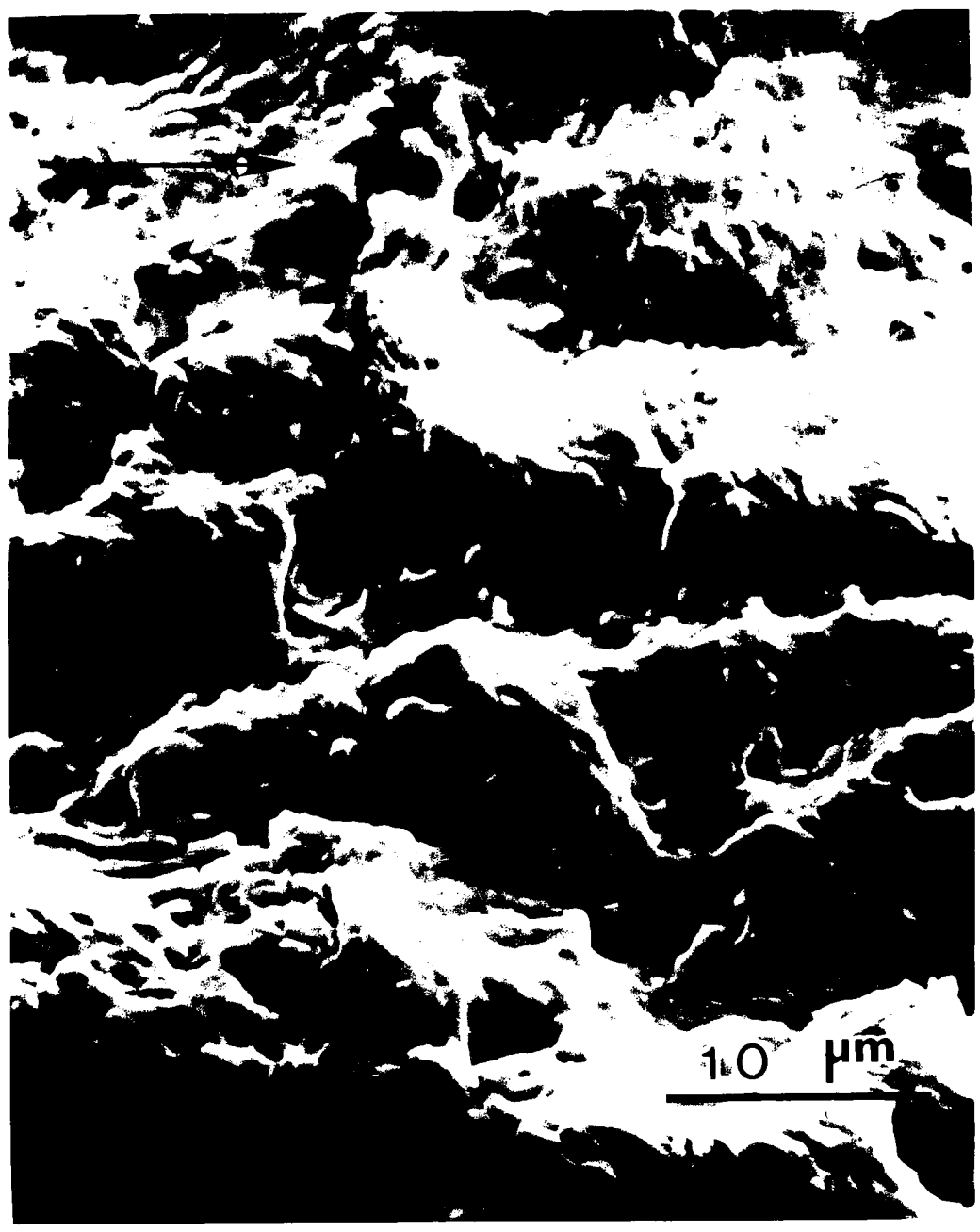

Figure 3.23. SEM fractograph of alloy 25 in the annealed condition showing fatigue striations along with high plastic deformation. The arrow indicate the crack growth direction.

4. CONCLUSIONS

Fatigue and corrosion fatigue tests of Be-Cu spring materials in the annealed, cold rolled, and aged conditions were conducted in ambient air and aqueous salt solution for smooth and notched specimen configurations with the stress ratio of 0.1. Test frequencies were 50 Hz and 1 Hz for air and corrosion fatigue tests, respectively. Based on these results, the conclusions are:

Ambient Air Environment

1. For smooth specimens of alloy 25, fatigue strength increases with increasing tensile strength. This effect diminishes as fatigue cycles increase from 10^4 to 10^6 cycles. Notched specimens of alloy 25 show the same trend but with a reduced influence of strength.

2. Normalized fatigue strength, $\Delta S/UTS$, for both notched and smooth specimens of alloy 25 show annealed material to be superior to stronger materials at all cyclic lives. Notch blunting and cyclic hardening are considered as likely explanations for this behavior at short and long lives, respectively.

3. Fatigue notch sensitivity, as measured by K_f for K_t=2.73, increases with increasing strength and cyclic life.

4. Crack initiation is the dominant fatigue process for Be-Cu spring materials for the present test conditions.

Aqueous Environment

5. For smooth specimens of annealed and cold rolled and aged alloy 25, environmental sensitivity (reduction in fatigue strength) increases as strength and cyclic life increases.

6. Notched specimens of annealed and cold rolled and aged alloy 25 exhibited about the same fatigue life in ambient and equeous environments.

7. The environmental sensitivity of alloy 25 in present tests of smooth specimens conflicts with other results suggesting Be-Cu alloys are insensitive to environment. The source of this difference is probably the lower frequency in these tests, i.e., 1 versus 20 Hz.

5. REFERENCES

1. Metals Handbook, ASM, Metals Park, OH, 9th Ed, Vol. 3, 1980, p. 589.

2. D. J. Duquette, "Encyclopedia of Materials Science and Engineering", MIT, Cambrige, MA, 1986, p. 878.

3. T. S. Sudarshan, T. S. Sirvatsan, and D. P. Harvey, Eng. Frac. Mech., Vol. 36, No. 6, 827(1990).

4. V. I. Pokhmurskii, Proc. 1st USSR-UK Seminar on Corrosion Fatigue of Metals, Met. Soc., London, 47(1983).

5. H. J. Gough and D. J. Sopwith, J. Inst. Met., Lx(1), 143(1937).

6. J. T. Richards, Corrosion, Vol. 9, 359(1953).

7. W. C. Stewart and W. L. Williams, Proc. ASTM, 836(1946).

8. C. E. Jaske, J. H. Payer, and V. S. Balnit, "Corrosion Fatigue of Metals in Marine Environments", Metals and Ceramic Information Center, NY, 1981, p. 133.

9. N. Thompson and N. H. Wadworth, Phil. Mag. Suppl., 7, 72(1958).

10. J. C. Grosskreutz and P. Waldow, Acta Metall., Vol. 11, 717(1963).

11. W. J. Pulmbridge and D. A. Ryder, Metall. Rev. No. 136, 119(1969).

12. W. A. Wood, Bull. Inst. Met., Vol. 3, 5(1955).

13. N. Thompson, N. H. Wadworth, and N. Loat, Phil. Mag., Vol. 1, 113(1956).

14. H. E. Frankel, J. A. Bennet, and W. A. Pennington, Trans. ASM, 52, 257(1960).

15. P. H. Frith, J. Ir. St. Inst., 159, 385(1948).

16. G. E. Dieter, "Mechanical Metallurgy", Mc Grow Hill, NY, 1986, p. 394.

17. D. J. Duquette, Proc. 2nd Int. Conf. on environmental Degradation of Engineering Materials, VPI, 131(1981).

18. R. W. Hertzberg, "Deformation and Fracture Mechanics of Engineering Materials" Wiley, NY, 1989, p. 562.

19. C. Laird and D. J. Duquette, "Corrosion Fatigue: Chemistry, Mechanics, and Microstructure", National Association of corrosion Engineers, TX, 88(1971).

20. H. N. Hahn and D. J. Duquette, Acta Metall., Vol. 26, 279(1978).

21. H. N. Hahn and D. J. Duquette, Metall. Trans., Vol. 10A, 1453(1979).

22. H. J. Gough, J. Inst. Met., 49, 17(1932).

23. P. Mehdizadeh, R. L. Mc Glasson, and J. E. Landers, Corrosion, Vol. 22, No. 12, 325(1966).

24. Duquette and H. H. Uhlig, Trans. ASM, Vol. 61, 449(1968).

25. D. J. Duquette and H. H. Uhlig, Trans. ASM, Vol. 62, 839(1969).

26. N. H. Polakowski and A. Palchoudhuri, ASTM, Preprint No. 74, 701(1954).

27. R. W. Smith, M. H. Hirschberg, and S. S. Manson, NASA TN D-1574, April 1963.

28. J. Awatani, K. Katagiri, A. Omura, and T. Shiraishi, Metall. Trans., Vol. 6A, 1029(1975).

29. J. Lindigkeit, A. Gysler, and G. Lutjering, Z. Metalkude, Bd. 72, 322(1981).

30. H. Masuda and D. J. Duquette, Metal Trans., Vol. 6A, 87(1985).

31. R. E. Peterson, "Stress Concentration Factors", Wiley, NY, 1974.

32. R. W. Hertzberg, "Deformation and Fracture Mechanics of Engineering Materials" Wiley, NY, 1989, p. 246.

33. N. E. Frost, K. J. Marsh, and L. P. Pook, "Metal Fatigue", Clarendon Press, Oxford, 1974, p. 143.

34. J. A. Collins, "Failure of Materials in Mechanical Design", Wiley, NY, 1974, p. 143.

35. R. W. Hertzberg, "Deformation and Fracture Mechanics of Engineering Materials" Wiley, NY, 1989, p. 469.

36. G. A. Miller, Research Report SG83-1, AISI, Washington, 1983.

37. ASTM Standard B194-88, 1988 Annual Book of ASTM Standards, Vol. 02.01, Philadelphia, PA, 1988, p. 314.

38. ASTM Standard B 534, 1988 Annual Book of ASTM Standards, Vol. 02.01, Philadelphia, PA, 1988, p. 604.

39. ASTM Standard B 601-83a, 1988 Annual Book of ASTM Standards, Vol. 02.01, Philadelphia, PA, 1988, p. 673.

40. ASTM Standard E 8-87a, 1988 Annual Book of ASTM Standards, Vol. 03.01, Philadelphia, PA, 1988, p. 121.

41. ASTM Standard E 466-82, 1988 Annual Book of ASTM Standards, Vol. 03.01, Philadelphia, PA, 1988, p. 532.

42. R. B. Jones and V. A. Phillips, Trans. ASM, Vol. 53, 603(1961).

43. G. Oates and D. V. Wilson, Acta Metall., Vol. 12, 21(1964).

44. D. V. Wilson and J. K. Tromans, Acta Metall., Vol. 18, 1197(1970).

45. G. A. Miller and H. S. Reemsnyder, SAE Technical Paper no. 830176, SAE, Warrendale, PA, 43, 1983.

46. H. R. Azimi, M.S. Thesis, Lehigh University, Bethlehem, PA, 1991.

47. D. Broek, Int. Metall. Rev., Vol. 19, 135(1974).

VITA

Reza Bagheri, son of Mansoor and Tallieh Bagheri, was born in Tehran, Iran, on July 16, 1961. He graduated from Kharazmi high school in 1979 and received his B.S. degree in Metallurgical Engineering from Sharif University of Technology in June, 1987.

He was employed by the Department of Metallurgical Engineering of Sharif University as a research engineer for two years after his graduation. Since January 1990, he has been conducting graduate research in Materials Science and Engineering at Lehigh University under the direction of Dr. Gary A. Miller.